

**STRUCTURAL DAMAGE DETECTION USING FREQUENCY
RESPONSE FUNCTIONS**

A Thesis

by

SELCUK DINCAL

Submitted to the Office of Graduate Studies of
Texas A&M University
in partial fulfillment of the requirements for the degree of

MASTER OF SCIENCE

December 2005

Major Subject: Civil Engineering

**STRUCTURAL DAMAGE DETECTION USING FREQUENCY
RESPONSE FUNCTIONS**

A Thesis

by

SELCUK DINCAL

Submitted to the Office of Graduate Studies of
Texas A&M University
in partial fulfillment of the requirements for the degree of

MASTER OF SCIENCE

Approved by:

Chair of Committee, Anne M. Raich
Committee Members, Harry L. Jones
N.K. Anand
Head of Department, David V. Rosowsky

December 2005

Major Subject: Civil Engineering

ABSTRACT

Structural Damage Detection Using Frequency

Response Functions. (December 2005)

Selcuk Dincal, B.S., Osmangazi University, Eskisehir, Turkey

Chair of Advisory Committee: Dr. Anne M. Raich

This research investigates the performance of an existing structural damage detection method (SDIM) when only experimentally-obtained measurement information can be used to calculate the frequency response functions used to detect damage. The development of a SDIM that can accurately identify damage while processing measurements containing realistic noise levels and overcoming experimental modeling errors would provide a robust method for identifying damage in the larger, more complex structures found in practice. The existing SDIM program, GaDamDet, uses an advanced genetic algorithm, along with a two-dimensional finite element model of the structure, to identify the location and the severity of damage using the linear vibration information contained in frequency response functions (FRF) as response signatures. Datagen is a Matlab program that simulates the three-dimensional dynamic response of the four-story, two-bay by two-bay UBC test structure built at the University of British Columbia. The dynamic response of the structure can be obtained for a range of preset damage cases or for any user-defined damage case. Datagen can be used to provide the FRF measurement information for the three-dimensional test structure. Therefore, using the FRF measurements obtained from the UBC test structure allows for a more realistic evaluation of the performance of the SDIM provided by GaDamDet as the impact on performance of more realistic noise and model errors can be investigated. Previous studies evaluated the performance of the SDIM using only simulated FRF measurements obtained from a two-dimensional structural model. In addition, the disparity between the

two-dimensional model used by the SDIM used to identify damage and the measurements obtained from the three-dimensional test structure is analyzed.

The research results indicate that the SDIM is able to accurately detect structural damage to individually damaged members or to within a damaged floor, with few false damages identified. The SDIM provides an easy to use, visual, and accurate algorithm and its performance compares favorably to performance of the various damage detection algorithms that have been proposed by researchers to detect damage in the three-dimensional structural benchmark problem.

DEDICATION

To my parents Sevki and Ayla Dincal,
and my dear Paola

ACKNOWLEDGEMENTS

I would like to thank to Dr. Anne M. Raich, for the guidance and support that she has given me throughout the research and Dr. Harry Jones and Dr. N.K. Anand for their willingness to be on the advisory committee as well as the contributions they have made. Special thanks to Dr. Tamas Liskai and Dr. Norris Stubbs for their inspiring advice and critiques. This research wouldn't have been completed without their valuable suggestions.

Finally, I would like to thank and dedicate this work to my parents Sevki and Ayla Dincal and my dear Paolita that always has been there for me.

TABLE OF CONTENTS

	Page
ABSTRACT	iii
DEDICATION	v
ACKNOWLEDGEMENTS	vi
TABLE OF CONTENTS	vii
LIST OF FIGURES.....	x
LIST OF TABLES	xvi
1 INTRODUCTION.....	1
1.1 Overview	1
1.2 Research Objectives	1
1.3 Background.....	2
1.3.1 Frequency Response Functions for Damage Detection	3
1.3.2 Description of UBC Structural Benchmark Problem	4
1.4 Organization of the Thesis.....	6
2 HYBRID STRUCTURAL DAMAGE IDENTIFICATION METHODOLOGY.....	8
2.1 Description of the Structural Damage Identification Program GaDamDet.....	8
2.1.1 Detecting Structural Damage Using GaDamDet.....	8
2.1.2 Running GaDamDet	11
2.2 Description of the Experimental Response Measurement Program Datagen.....	16
2.2.1 Definition of UBC Test Structure	19
2.3 Discussion of the Hybrid Structural Damage Identification Method Proposed	21
2.3.1 Modifications Required in the Finite Element Model Used by GaDamdet.....	22
2.3.2 Modifications Required in the Measurement/Excitation Pairs.....	24
2.3.3 Required Input/Output Parameters in Datagen	25
3 FREQUENCY RESPONSE FUNCTIONS	28
3.1 Random Data	28
3.1.1 Stationary Random Data	29

	Page
3.1.1.1 Ergodic Stationary Random Data	30
3.2 Analysis of Random Data.....	30
3.3 Input/Output Relations	33
3.4 Basic Dynamic Characteristics.....	34
3.5 Frequency Response Functions	37
3.6 Single-Input/Output Relationships	38
3.6.1 Single-Input/Single-Output Models	38
3.6.2 Single-Input/Multiple-Output Models.....	43
3.7 Multiple-Input/Output Relationships	45
3.7.1 Multiple-Input/Single-Output Models.....	45
3.7.1.1 Two-Input/One-Output Models	50
3.7.1.2 Multiple Coherence Functions.....	53
3.7.1.3 Conditioned Spectral Density Functions	54
3.7.1.4 Partial Coherence Functions	58
3.7.2 General and Conditioned Multiple-Input Models	59
3.7.2.1 Algorithm for Conditioned Spectra and Frequency Response Functions	62
Spectral Density and Frequency Response Functions Using Matrix Calculations	65
3.7.2.3 Partial and Multiple Coherence Functions	67
4 ANALYSIS MODELS FOR BENCHMARK TEST CASES	70
4.1 Single-Input/Multiple-Output Model	73
4.2 Multiple-Input/Multiple-Output Model.....	76
5 RESULTS AND DISCUSSIONS	84
5.1 Single-Input/Multiple-Output Model	85
5.1.1 Case 3: 1 st Story Braces Are Damaged	85
5.1.1.1 All Four Modes Are Used for Damage Detection	87
5.1.1.2 The Last Mode Is Omitted for Damage Detection	90
5.1.2 Case 3: 1 st - 3 rd Story Braces Are Damaged	92
5.1.2.1 All Four Modes Are Used for Damage Detection	95
5.1.2.2 The Last Two Modes Are Omitted for Damage Detection	97
5.1.3 Case 3: 2 nd Story Braces Are Damaged	100
5.1.4 Case 4: 1 st Story Braces Are Damaged.....	101
5.1.5 Case 4: 1 st - 3 rd Story Braces Are Damaged	104
5.1.6 Case 5: 1 st Story Braces Are Damaged.....	106
5.1.7 Case 5: 1 st - 3 rd Story Braces Are Damaged	110
5.2 Multiple-Input/Single-Output Model	113
5.2.1 Case 1: 1 st Story Braces Are Damaged	113

	Page
5.2.1.1	The Measurement Is Taken From the First Floor (at Node 7)..... 113
5.2.1.2	The Measurement Is Taken From The Second Floor (at Node 8) 116
5.2.2	Case 1: 1 st - 3 rd Story Braces Are Damaged 118
5.3	Multiple-Input/Multiple-Output Model..... 120
5.3.1	Case 1: 1 st Story Braces Are Damaged 121
5.3.1.1	All Four Modes Are Used for Damage Detection 124
5.3.1.2	The Last Mode Is Omitted for Damage Detection 126
5.3.2	Case 1: 1 st - 3 rd Story Braces Are Damaged 127
5.3.2.1	All Four Modes Are Used for Damage Detection 130
5.3.2.2	First Two Modes Are Used for Damage Detection 132
5.3.3	Case 1: 3 rd Story Braces Are Damaged 134
5.3.4	Case 2: 1 st Story Braces Are Damaged 135
5.3.5	Case 2: 1 st - 3 rd Story Braces Are Damaged 138
5.4	Effect of Noise on Performance of the SDIM 141
5.4.1	SIMO Model: 1 st Story Braces Are Damaged Using Case 3 (10% Noise)..... 142
5.4.2	MISO Model: 1 st Story Braces Are Damaged Using Case 1 (10% Noise)..... 144
5.4.3	MIMO Model: 1 st Story Braces Are Damaged Using Case 1 (10% Noise)..... 147
6	SUMMARY AND CONCLUSIONS..... 150
6.1	Future Recommendations..... 152
	REFERENCES 154
	APPENDIX A 157
	APPENDIX B 162
	VITA 164

LIST OF FIGURES

	Page
Figure 2.1 Main Menu Structure of <i>GaDamDet</i> Program	11
Figure 2.2 Settings Menu and Its Toolbar.....	12
Figure 2.3 Finite Element Model Input and Matlab Measurement Data Files.....	13
Figure 2.4 Genetic Algorithm Parameter Sheet	14
Figure 2.5 Structure Plot Option in <i>GaDamDet</i>	15
Figure 2.6 Damage Cases Defined by <i>Datagen</i> for the UBC Benchmark Problem...	17
Figure 2.7 <i>Datagen</i> Case IDs.....	18
Figure 2.8 <i>Datagen</i> Parameter Sheet	19
Figure 2.9 UBC Test Structure.....	20
Figure 2.10 Input/Output Parameters for the Multiple-Input/Multiple-Output Model (Only in Weak Direction)	26
Figure 2.11 Input/Output Parameters for the Single-Input/Multiple-Output Model (Both in Weak and Strong Direction)	26
Figure 3.1 Single-Input/Single-Output System with Output Noise	33
Figure 3.2 Single-Input/Multiple-Output System with Output Noise.....	35
Figure 3.3 Single-Input/Multiple-Output System	44
Figure 3.4 Multiple-Input/Single-Output System	46
Figure 3.5 Two-Input/One-Output System with Output Noise.....	51
Figure 3.6 Decomposition of $x_2(t)$ from $x_1(t)$	55
Figure 3.7 Two-Input/One-Output Model with Mutually Uncorrelated Inputs	57
Figure 3.8 Multiple-Input Model for Arbitrary Inputs.....	60

	Page
Figure 3.9 Multiple-Input Model for Ordered Conditioned Inputs	61
Figure 4.1 Node Numbering for 2-D Finite Element Model.....	70
Figure 4.2 Element Numbering for 2-D Finite Element Model	70
Figure 4.3 Input/Output Locations for the Single-Input/Multiple-Output Model.....	72
Figure 4.4 Input/Output Locations for the Multiple-Input/Multiple-Output Model ..	72
Figure 4.5 Cross-Spectrum Function Between Force Input at Roof Level and Acceleration Output at the First Floor in the Weak Direction	74
Figure 4.6 Frequency Response Function Between Force Input at Roof Level and Acceleration Output at the First Floor in the Weak Direction	75
Figure 4.7 Ordinary Coherence Function Between Force Input at Roof Level and Acceleration Output at the First Floor in the Weak Direction	75
Figure 4.8 Ordinary Coherence Function Between Force Input at the First and Second Floor	76
Figure 4.9 Ordinary Coherence Function Between Force Input and Acceleration Output at the First Floor	77
Figure 4.10 Multiple Coherence Function Between the Output (First Floor Acceleration) and the Given Inputs (Forces in each Story)	78
Figure 4.11 FRF for 12/7 Excitation/Masurement Pair for the MIMO Problem	80
Figure 4.12 FRF for 13/8 Excitation/Masurement Pair for the MIMO Problem	81
Figure 4.13 FRF for 13/7 Excitation/Masurement Pair for the MISO Problem	82
Figure 4.14 FRF for 14/7 Excitation/Masurement Pair for the MISO Problem	83
Figure 5.1 FRF for the 1 st Floor – 1 st Story Braces Are Broken SIMO – 12 DOF Symmetric Model	85
Figure 5.2 FRF for the 2 nd Floor – 1 st Story Braces Are Broken SIMO – 12 DOF Symmetric Model	86

	Page
Figure 5.3 FRF for the 3 rd Floor – 1 st Story Braces Are Broken SIMO – 12 DOF Symmetric Model	86
Figure 5.4 FRF for the 4 th Floor – 1 st Story Braces Are Broken SIMO – 12 DOF Symmetric Model	87
Figure 5.5 Simulated vs. Detected Damages for Trial #1	88
Figure 5.6 Simulated vs. Detected Damages for Trial #1 with Hillclimbing #1867	90
Figure 5.7 Simulated vs. Detected Damages for Trial #2 with Hillclimbing #739	92
Figure 5.8 FRF for the 1 st Floor – 1 st - 3 rd Story Braces Are Broken SIMO – 12 DOF Symmetric Model	93
Figure 5.9 FRF for the 2 nd Floor – 1 st - 3 rd Story Braces Are Broken SIMO – 12 DOF Symmetric Model	93
Figure 5.10 FRF for the 3 rd Floor – 1 st - 3 rd Story Braces Are Broken SIMO – 12 DOF Symmetric Model	94
Figure 5.11 FRF for the 4 th Floor – 1 st - 3 rd Story Braces Are Broken SIMO – 12 DOF Symmetric Model	94
Figure 5.12 Simulated vs. Detected Damages for Trial #3 with Hillclimbing #178	96
Figure 5.13 Simulated vs. Detected Damages for Trial #4	99
Figure 5.14 Simulated vs. Detected Damages for Trial #4 with Hillclimbing #1489	99
Figure 5.15 Simulated vs. Detected Damages for Trial #5	101
Figure 5.16 FRF for the 1 st Floor – 1 st Story Braces Are Broken SIMO – 12 DOF Asymmetric Model	102
Figure 5.17 Simulated vs. Detected Damages for Trial #6 with Hillclimbing #667	104

	Page
Figure 5.18 FRF for the 1 st Floor – 1 st - 3 rd Story Braces Are Broken SIMO – 12 DOF Asymmetric Model	105
Figure 5.19 Simulated vs. Detected Damages for Trial #7 with Hillclimbing #580	107
Figure 5.20 FRF for the 1 st Floor – 1 st Story Braces Are Broken SIMO – 120 DOF Asymmetric Model	107
Figure 5.21 Simulated vs. Detected Damages for Trial #8 with Hillclimbing #519	109
Figure 5.22 FRF for the 1 st Floor – 1 st - 3 rd Story Braces Are Broken SIMO – 120 DOF Asymmetric Model	110
Figure 5.23 Simulated vs. Detected Damages for Trial #9 with Hillclimbing #1575	112
Figure 5.24 FRF for the 1 st Floor – 1 st Story Braces Are Broken MISO – 12 DOF Symmetric Model	114
Figure 5.25 Simulated vs. Detected Damages for Trial #10 with Hillclimbing #8693	116
Figure 5.26 Simulated vs. Detected Damages for Trial #11 with Hillclimbing #160	118
Figure 5.27 FRF for the 1 st Floor – 1 st - 3 rd Story Braces Are Broken MISO – 12 DOF Symmetric Model	119
Figure 5.28 Simulated vs. Detected Damages for Trial #12 with Hillclimbing #9903	121
Figure 5.29 FRF for the 1 st Floor – 1 st Story Braces Are Broken MIMO – 12 DOF Symmetric Model	122
Figure 5.30 FRF for the 2 nd Floor – 1 st Story Braces Are Broken MIMO – 12 DOF Symmetric Model	122
Figure 5.31 FRF for the 3 rd Floor – 1 st Story Braces Are Broken MIMO – 12 DOF Symmetric Model	123

	Page
Figure 5.32 FRF for the 4 th Floor – 1 st Story Braces Are Broken MIMO – 12 DOF Symmetric Model	123
Figure 5.33 Simulated vs. Detected Damages for Trial #13 with Hillclimbing #3395	125
Figure 5.34 Simulated vs. Detected Damages for Trial #14 with Hillclimbing #1232	127
Figure 5.35 FRF for the 1 st Floor – 1 st - 3 rd Story Braces Are Broken MIMO – 12 DOF Symmetric Model	128
Figure 5.36 FRF for the 2 nd Floor – 1 st - 3 rd Story Braces Are Broken MIMO – 12 DOF Symmetric Model	128
Figure 5.37 FRF for the 3 rd Floor – 1 st - 3 rd Story Braces Are Broken MIMO – 12 DOF Symmetric Model	129
Figure 5.38 FRF for the 4 th Floor – 1 st - 3 rd Story Braces Are Broken MIMO – 12 DOF Symmetric Model	129
Figure 5.39 Simulated vs. Detected Damages for Trial #15 with Hillclimbing #10511	131
Figure 5.40 Simulated vs. Detected Damages for Trial #16 with Hillclimbing #5039	133
Figure 5.41 Simulated vs. Detected Damages for Trial #17 with Hillclimbing #1266	135
Figure 5.42 FRF for the 1 st Floor – 1 st Story Braces Are Broken MIMO – 120 DOF Symmetric Model	136
Figure 5.43 Simulated vs. Detected Damages for Trial #18 with Hillclimbing #309	138
Figure 5.44 FRF for the 1 st Floor – 1 st - 3 rd Story Braces Are Broken MIMO – 120 DOF Symmetric Model	139
Figure 5.45 Simulated vs. Detected Damages for Trial #19 with Hillclimbing #58	141

	Page
Figure 5.46 FRF for the 1 st Floor – 1 st Story Braces Are Broken SIMO – 12 DOF Symmetric Model (10% Noise).....	142
Figure 5.47 Simulated vs. Detected Damages for Trial #20 with Hillclimbing #4976	144
Figure 5.48 FRF for the 1 st Floor – 1 st Story Braces Are Broken MISO – 12 DOF Symmetric Model (10% Noise).....	145
Figure 5.49 Simulated vs. Detected Damages for Trial #21 with Hillclimbing #4083	147
Figure 5.50 FRF for the 4 th Floor – 4 th Story Braces Are Broken MIMO – 12 DOF Symmetric Model (10% Noise).....	148
Figure 5.51 Simulated vs. Detected Damages for Trial #22	149
Figure A.1 Sample Input File of a SIMO Problem for the <i>ModalFEM</i> Utility Program	161

LIST OF TABLES

		Page
Table 2.1	The Section Properties of the Benchmark Structure	21
Table 5.1	GA Parameters Used	84
Table 5.2	SDIM Results for 1 st Story Braces Damaged Using 4 FRFs – SIMO Case 3, All Four Modes Are Used	88
Table 5.3	SDIM Results for 1 st Story Braces Damaged Using 4 FRFs – SIMO Case 3, All Four Modes Are Used, After Hillclimbing #1867	89
Table 5.4	SDIM Results for 1 st Story Braces Damaged Using 4 FRFs – SIMO Case 3, Last Mode Is Omitted	91
Table 5.5	SDIM Results for 1 st Story Braces Damaged Using 4 FRFs – SIMO Case 3, Last Mode Is Omitted, After Hillclimbing #739	91
Table 5.6	SDIM Results for 1 st and 3 rd Story Braces Damaged Using 4 FRFs – SIMO Case 3, All Four Modes Are Used	95
Table 5.7	SDIM Results for 1 st and 3 rd Story Braces Damaged Using 4 FRFs – SIMO Case3, All Four Modes Are Used, After Hillclimbing #178	95
Table 5.8	SDIM Results for 1 st and 3 rd Story Braces Damaged Using 4 FRFs – SIMO Case 3, Last Two Modes Are Omitted	97
Table 5.9	SDIM Results for 1 st and 3 rd Story Braces Damaged Using 4 FRFs – SIMO Case 3, Last Two Modes Are Omitted, After Hillclimbing #1489	98
Table 5.10	SDIM Results for 2 nd Story Braces Damaged Using 4 FRFs – SIMO Case 3	100
Table 5.11	SDIM Results for 1 st Story Braces Damaged Using 4 FRFs – SIMO Case 4	103
Table 5.12	SDIM Results for 1 st Story Braces Damaged Using 4 FRFs – SIMO Case 4, After Hillclimbing #1867	103
Table 5.13	SDIM Results for 1 st and 3 rd Story Braces Damaged Using 4 FRFs – SIMO Case 4	105

	Page
Table 5.14 SDIM Results for 1 st and 3 rd Story Braces Damaged Using 4 FRFs – SIMO Case 4, After Hillclimbing #580	106
Table 5.15 SDIM Results for 1 st Story Braces Damaged Using 4 FRFs – SIMO Case 5	108
Table 5.16 SDIM Results for 1 st Story Braces Damaged Using 4 FRFs – SIMO Case 5, After Hillclimbing #519	109
Table 5.17 SDIM Results for 1 st and 3 rd Story Braces Damaged Using 4 FRFs – SIMO Case 5	111
Table 5.18 SDIM Results for 1 st and 3 rd Story Braces Damaged Using 4 FRFs – SIMO Case 5, After Hillclimbing #1575	111
Table 5.19 SDIM Results for 1 st Story Braces Damaged Using 4 FRFs – MISO Case 1, Accelerometer Is at Node 7	115
Table 5.20 SDIM Results for 1 st Story Braces Damaged Using 4 FRFs – MISO Case 1, Accelerometer Is at Node 7, After Hillclimbing #8693	115
Table 5.21 SDIM Results for 1 st Story Braces Damaged Using 4 FRFs – MISO Case 1, Accelerometer Is at Node 8	117
Table 5.22 SDIM Results for 1 st Story Braces Damaged Using 4 FRFs – MISO Case 1, Accelerometer Is at Node 8, After Hillclimbing #160	117
Table 5.23 SDIM Results for 1 st and 3 rd Story Braces Damaged Using 4 FRFs – MISO Case 1, Accelerometer Is at Node 7	120
Table 5.24 SDIM Results for 1 st and 3 rd Story Braces Damaged Using 4 FRFs – MISO Case 1, Accelerometer Is at Node 7, After Hillclimbing #9903	120
Table 5.25 SDIM Results for 1 st Story Braces Damaged Using 4 FRFs – MIMO Case 1, All Four Modes Are Used	124
Table 5.26 SDIM Results for 1 st Story Braces Damaged Using 4 FRFs – MIMO Case 1, All Four Modes Are Used, After Hillclimbing #3395	124
Table 5.27 SDIM Results for 1 st Story Braces Damaged Using 4 FRFs – MIMO Case 1, The Last Mode Is Omitted.....	126

	Page
Table 5.28 SDIM Results for 1 st Story Braces Damaged Using 4 FRFs – MIMO Case 1, The Last Mode Is Omitted, After Hillclimbing #1232.....	126
Table 5.29 SDIM Results for 1 st and 3 rd Story Braces Damaged Using 4 FRFs – MIMO Case 1, All Four Modes Are Used	130
Table 5.30 SDIM Results for 1 st and 3 rd Story Braces Damaged Using 4 FRFs – MIMO Case 1, All Four Modes Are Used, After Hillclimbing #10511	131
Table 5.31 SDIM Results for 1 st and 3 rd Story Braces Damaged Using 4 FRFs – MIMO Case 1, First Two Modes Are Used	132
Table 5.32 SDIM Results for 1 st and 3 rd Story Braces Damaged Using 4 FRFs – MIMO Case 1, First Two Modes Are Used, After Hillclimbing #5039	133
Table 5.33 SDIM Results for 3 rd Story Braces Damaged Using 4 FRFs – MIMO Case 1	134
Table 5.34 SDIM Results for 3 rd Story Braces Damaged Using 4 FRFs – MIMO Case 1, After Hillclimbing #1266	134
Table 5.35 SDIM Results for 1 st Story Braces Damaged Using 4 FRFs – MIMO Case 2	136
Table 5.36 SDIM Results for 1 st Story Braces Damaged Using 4 FRFs – MIMO Case 2, After Hillclimbing #309	137
Table 5.37 SDIM Results for 1 st and 3 rd Story Braces Damaged Using 4 FRFs – MIMO Case 2.....	139
Table 5.38 SDIM Results for 1 st and 3 rd Story Braces Damaged Using 4 FRFs – MIMO Case 2, After Hillclimbing #58.....	140
Table 5.39 SDIM Results for 1 st Story Braces Damaged Using 4 FRFs (10% Noise) – SIMO Case 3	143
Table 5.40 SDIM Results for 1 st Story Braces Damaged Using 4 FRFs (10% Noise) – SIMO Case 3, After Hillclimbing #4976.....	143
Table 5.41 SDIM Results for 1 st Story Braces Damaged Using 4 FRFs (10% Noise) – MISO Case 1	146

	Page
Table 5.42 SDIM Results for 1 st Story Braces Damaged Using 4 FRFs (10% Noise) – MISO Case 1, After Hillclimbing #4083.....	146
Table 5.43 SDIM Results for 1 st Story Braces Damaged Using 4 FRFs (10% Noise) – MIMO Case 1	149
Table A.1 Cards That Can be Used in the Text Input File (*.inp) for the <i>ModalFEM</i> Utility Program	157
Table B.1 List of Files in the Datagen Package	162
Table B.2 List of Input Parameters in the Datagen Package.....	162
Table B.3 List of Output Parameters in the Datagen Package	163

1 INTRODUCTION

1.1 Overview

Detecting structural damage using the information contained in vibration signatures has become more widely accepted by researchers and practitioners due to the availability of efficient and economical analysis methods and measurement systems. Vibration-based structural identification methods (SDIM) can provide global identification methods that also minimize the level of destructive impact on structural integrity that may occur in the search for damage. In comparison, often only limited information can be obtained concerning structural damage using local non-destructive damage detection techniques, which include radiographs, magnetic and ultrasonic methods. In addition, in order to use local techniques for health monitoring, typically the approximate damage location must be known which makes these methods highly unsuitable for automated health monitoring systems. Global damage detection methods have the potential to provide information throughout the life-cycle of a structure, while local damage methods are usually suited to checking the immediate condition of specific structural members or connections after a natural hazard like an earthquake or hurricane.

1.2 Research Objectives

This research evaluates the performance of an existing structural damage identification program, GaDamDet, in identifying damage globally for a large-scale experimental structure. The hybrid SDIM proposed uses the frequency response functions (FRF) obtained from the first phase of the benchmark structural health monitoring (SHM) problem as input parameters in the GaDamDet structural damage detection program.

Therefore, this research investigates several complex issues related to signal processing, including input/output relationships and data processing.

Different analytical models of the three-dimensional test structure are examined in order to study the effects that model complexity and model error have on the SDIM's performance. The loss or gain of useful information is also examined by choosing partial or full sensor locations in the system. The performance of the proposed hybrid SDIM is compared to the performance of different SDIMs developed by other researchers on the same benchmark problem and to the performance of GaDamDet using the program's original features and models. The measurements taken from the UBC damaged structure are available and are used to validate the responses obtained by Datagen. Evaluating the performance of the SDIM using the FRFs obtained from the UBC test structure will allow conclusions to be made concerning the potential benefits of using the GaDamDet SDIM in real-time monitoring applications of large, more realistic structural systems.

This thesis also provides useful tools regarding random data analysis by developing methods for obtaining frequency response functions from the force and response records provided by the UBC benchmark problem for any damage condition.

1.3 Background

A vibration-based damage detection algorithm is used in this research. The idea behind this technique is that the changes in a structure's physical properties will cause changes in the structure's dynamic response properties, which include natural frequencies, modal shapes and frequency response functions of the structure.

A literature review of vibration-based damage identification methods was provided by Doebling *et al* in 1996 and 1998. Several methods that include using changes in mode shapes, changes in natural frequencies, measurements of flexibility to detect damage in structures are explained in these research reviews.

Rytter (1993) provided a system in which a SDIM can be classified into one of four levels according to their capabilities. Level 1 concerns the capability to detect

damage but only by relaying information about the existence of damage in structures. Level 2 concerns damage localization. A Level 2 method provides information about the possible damage locations. Level 3 concerns assessment and these methods are capable of estimating the severity of the damage in addition to the previous information. Level 4 methods involve prediction. These methods would be capable of estimating the remaining life of a structure in addition to locating and quantifying the damage.

In addition to the level of damage detection provided, different SDIMs can also be classified according to the parameters used such as the response or static measurement information used (either in time domain or frequency domain), the type of excitation or loading provided (known or unknown), and the type of optimization method or direct method used to identify the location and/or extent of damage.

Liszkai and Raich (2003) proposed a FRF-based SDIM which is examined further in this thesis for damage detection. The advantages of using FRF data over modal parameters are that FRF data can be measured directly on structures without any intermediate steps and that it provides information over a frequency range instead of only at certain frequencies. In the FRF-based SDIM program, the damage detection problem is formulated as an optimization problem, which is solved using an Implicit Redundant Representation (IRR) GA due to the unstructured nature of damage detection (Liszkai, 2003). The unstructured problem stems from not knowing a priori the number of damages in addition to the location and severity of the damages.

1.3.1 Frequency Response Functions for Damage Detection

Several researchers have relied on the used of FRF information for system identification and damage detection. Wang et al. (1997) used measured FRF data obtained before and after damage to develop an SDIM algorithm based on nonlinear perturbation equations. This method determined a damage vector that indicated both the location and magnitude of damage. The perturbation equations were weighted at selected locations and frequencies in order to reduce the effect of measurement errors. An iterative version of

the SDIM algorithm was also introduced to handle incomplete measurement cases. Lee and Shin (2002) introduced a FRF-based SDIM for beam structures using the dynamic equation motion for the intact and damaged beams in the continuous domain. Damages throughout the beam were described by a damage distribution function, which was assumed to have non-zero values at the damage locations. Instead of examining the whole domain of the problem, a reduced domain strategy was also developed that eliminated regions of possibly undamaged areas from the solution using an iterative technique. Thyagarajan et al. (1998) investigated the optimization of FRFs to diagnose damage using a minimum number of sensors. The proposed optimization problem was solved using a gradient-based optimization subroutine contained in the MATLAB (1999a) optimization toolbox. The SDIM technique developed is limited mainly to small structures due to its large computational expense. Sampaio et al. (1999) introduced the FRF Curvature Method as an extension of the Mode Shape Curvature Method proposed by Pandey et al. (1991). In the FRF Curvature Method damage is assessed by identifying the largest computed absolute difference between the mode shape curvatures of the damaged and undamaged structure. The difference between FRFs curvatures is used to detect, localize and quantify the damage. Marwala and Heyns (1998) used a combination of objective functions that used both FRF and modal information to minimize an error function using the MATLAB (1999a) optimization toolbox. Marwala (2000) presented a SDIM defined using a committee of neural networks that employed FRFs, modal parameters and wavelet transform data simultaneously to identify structural damage.

1.3.2 Description of UBC Structural Benchmark Problem

The joint International Association for Structural Control - American Society of Civil Engineers (IASC-ASCE) Structural Health Monitoring Task Group investigated a series of benchmark problem structures in order to provide a consistent forum to allow researchers to evaluate the performance of different SDIMs. Phase I of the study

involved simulating structural response using an analytical structural model subjected to different damage scenarios. Phase II considered the application of the proposed SDIMs to detect damage based on structural response data obtained experimentally. The test model used in both phases is a four-story, two-bay by two-bay steel-frame structure. Results obtained by different SDIMs have been presented in the literature and are collected on the Structural Health Monitoring Committee ASCE website. A special session was held to discuss the benchmark problem at the 14th ASCE Engineering Mechanics Conference in 2000 and at the Joint ASME-ASCE Mechanics and Materials Conference in 2001. A special issue in the Journal of Engineering Mechanics was prepared to present research results concerning the benchmark identification problem. An overview of the SDIMs previously researched for the benchmark problem is provided in the next few paragraphs.

Johnson, Lam, Katafygiotis and Beck (2000) presented detailed information concerning the properties of the structural members, imposed damage scenarios as well as detailed information concerning the simulation cases. Analysis of two different finite element models (12 and 120 DOF) was performed and the natural frequencies of the analytical models were presented in this study.

Au, Yuen and Beck (2000) applied a two-stage approach to identify damage. Natural Excitation Technique (NExT) was used to obtain the modal parameters of the system. An a priori probability density function (PDF) was first assumed for the mass and stiffness of the structure. A Bayesian statistical approach and the modal parameters obtained previously were used to update this prior PDF. By comparing the PDF of the stiffness of the system before and after damage, it was possible to detect the location and severity of the damage in a probabilistic manner.

The Damage Index Method is a SDIM developed by Park, Stubbs and Bolton (1998). This method detects, locates, and estimates the severity of damage using a damage indicator based on the relationship between the material stiffness properties of the undamaged and the damaged member of the structure. This method was used by Rodriguez and Barroso (2002) in conjunction with their proposed stiffness-mass ratios

method to estimate baseline modal parameters from damaged response data when a shear-beam model is used. These methods can identify damage locations in a structure to specific stories within the structure, since shear-beam models work with story stiffness changes.

Bernal and Gunes (2000) applied a multi-stage approach for detecting damage in the benchmark structure. As the first step, the modal characteristics were identified by using an Eigen System Realization Algorithm (ERA) with a Kalman observer or a subspace identification algorithm. The second and third steps involve locating damaged regions based on the identified flexibility matrix of the structure. Damage was then quantified by comparing the undamaged structure with the damaged structure.

Corbin, Hera and Hou (2000) proposed an application of wavelet analysis for damage detection in order to locate damage regions in structures. Damage and the moment that the damage occurred were detected by a spike or an impulse in a wavelet decomposition of the acceleration data. Quantification of the damage was not presented.

Dyke, Caicedo and Johnson (2000) used a combination of NExT and ERA methods for identification of modal parameters. Then, the optimal stiffness of structural elements was obtained using unconstrained nonlinear optimization. Changes in the stiffness coefficients indicated the location of damage, but the severity was difficult to quantify using this method.

1.4 Organization of the Thesis

This thesis is divided into six sections. Section 2 discusses the two programs used for evaluating the performance of the SDIM. Since the hybrid approach presented combines two programs, it is necessary to provide information about the parameters and input/output relationships of the programs. The finite element model used to define the benchmark structure is also explained in this section. Section 3 discusses how to obtain frequency response functions (FRF) from random data. After defining some basic concepts, mathematical formulations of the FRFs will be given. A simple algorithm is

also introduced in this section in order to compute FRFs for different input/output models. Section 4 focuses on how the force and acceleration signals obtained from Datagen are processed and how either a single input/multiple output (SIMO) or multiple input/multiple output (MIMO) problem is defined and solved in GaDamDet. Section 5 presents the SDIM results for the proposed hybrid approach and compares the results with other SDIMs developed by other researchers involved in the benchmark problem. The discussion includes an analysis of the SDIMs features, benefits, and limitations. In Section 6, a summary of the results is provided along with the conclusions made within the scope of this research. Future recommendations and future research extensions are also identified and discussed in this section.

2 HYBRID STRUCTURAL DAMAGE IDENTIFICATION METHODOLOGY

The hybrid structural damage identification methodology proposed links the FRF-based damage identification method provided by GaDamDet with measurement information obtained through Datagen for the UBC benchmark test structure. Before discussing the proposed hybrid approach in detail, the features and implementation details of the GaDamDet and the Datagen programs are discussed. Understanding the inputs and outputs of each program as well as parameters used will provide a better understanding and limitations of the hybrid SDIM methodology developed.

2.1 Description of the Structural Damage Identification Program GaDamDet

The SDIM provided by GaDamDet is based on the assumption that damage affects the stiffness of structural members. Therefore, damage can be detected globally by identifying changes in member stiffness, as any stiffness changes also affect the global dynamic response of the structure. A linear finite element model of the undamaged structure is also defined through a simple input card and is used as the baseline model for the SDIM. To detect damage, the stiffness parameters of the intact model are updated by the SDIM using an optimization method that seeks to match the analytically computed FRFs obtained from the updated baseline model to the measured FRFs obtained from the damaged structure.

2.1.1 *Detecting Structural Damage Using GaDamDet*

The theory behind the SDIM provided by GaDamDet is that minimizing the difference between the FRF matrices of the undamaged and the damaged structure captures both

the location and extent of damage. In order to formulate the damage detection problem as an optimization problem, an objective function is defined, that is minimized.

$$f = \sum_{k=k_1}^{k_n} \left(\int_{\varpi_0}^{\varpi} |\bar{A}_{jk}(\omega) - A_{jk}(\omega)| d\omega \right)^2 \quad (2.1)$$

where j is the excitation degree of freedom (DOF), k is the DOF where the response is measured, A_{jk} is the jk^{th} accelerance FRF in the finite element model, \bar{A}_{jk} is jk^{th} measured accelerance FRF, $k_1 \dots k_n$ are the DOF where measurements are taken, ϖ_0 and ϖ are the lower and upper frequencies of the measured frequency range, and the symbol $||$ indicates complex magnitude (Liszkai, 2003).

The analytical FRFs are found by inverting the dynamic stiffness matrix of the structure. If the system is excited by a set of sinusoidal forces with ω circular frequency, but with different amplitudes and phases, then the equations of motion can be written as:

$$\mathbf{M}\ddot{\mathbf{u}} + \mathbf{C}\dot{\mathbf{u}} + \mathbf{K}\mathbf{u} = \mathbf{f}_0 e^{-i\omega t} \quad (2.2)$$

where \mathbf{M} , \mathbf{C} and \mathbf{K} are the mass, damping, and stiffness matrices of the undamaged structure, \mathbf{u} is the displacement vector, ω is the circular natural frequency of excitation, \mathbf{f}_0 is the vector of complex forcing amplitudes, i is the imaginary unit, and t is time.

It is assumed that the solution of the above set of differential equations exists in the form

$$\mathbf{u} = \mathbf{z} e^{-i\omega t} \quad (2.3)$$

where \mathbf{z} is the vector of time independent complex amplitudes. The formal solution of equation (2.2) is obtained in the form.

$$\mathbf{z} = (\mathbf{K} - i\omega\mathbf{C} - \omega^2\mathbf{M})^{-1}\mathbf{f}_0 \equiv \mathbf{R}\mathbf{f}_0 \quad (2.4)$$

where the receptance matrix \mathbf{R} is defined as a function of ω .

$$\mathbf{R} = \mathbf{R}(\omega) \equiv (\mathbf{K} - i\omega\mathbf{C} - \omega^2\mathbf{M})^{-1} \quad (2.5)$$

The jk^{th} member of the receptance matrix represents the displacement response of the j^{th} DOF when the excitation is applied at the k^{th} DOF.

Each entry of the matrix of equation (2.4) is a function of ω and is also known as a frequency response function (FRF). Consequently, the receptance is a type of FRF too. From equation (2.3)

$$\dot{\mathbf{u}} \equiv \mathbf{v}e^{-i\omega t} = -i\omega\mathbf{z}e^{-i\omega t} \quad (2.6)$$

$$\ddot{\mathbf{u}} \equiv \mathbf{a}e^{-i\omega t} = -i\omega\mathbf{v}e^{-i\omega t} = -\omega^2\mathbf{z}e^{-i\omega t}$$

Using the above equations, the relationship between the receptance, mobility and accelerance matrices can be shown as:

$$\mathbf{V}(\omega) = -i\omega\mathbf{R}(\omega) \quad (2.7)$$

$$\mathbf{A}(\omega) = -\omega^2\mathbf{R}(\omega)$$

FRF matrices are commonly denoted with the notation of $\mathbf{H}(\omega)$. Receptance $\mathbf{R}(\omega)$, mobility $\mathbf{V}(\omega)$ or accelerance $\mathbf{A}(\omega)$ can be used as FRF matrices. The equations

derived for damage detection using the general FRF matrix are valid for any of the particular FRF matrices. Accelerance (inertance) will be used in this research in order to be consistent with the benchmark problem.

2.1.2 Running *GaDamDet*:

The *GaDamDet* program consists of three major modules:

1. Preprocessor for incorporating structural model, damage, and noise level information
2. Processor that includes the finite element, genetic algorithm (GA) and hillclimbing implementations,
3. A Postprocessor that include an easy to use graphical user interface.

These three modules were combined into a single program. The utility program, which generated simulated measurement data, is a separate program. The main program menu, settings menu and settings toolbar from *GaDamDet* are shown in Figures 2.1 and 2.2.



Figure 2.1 Main Menu Structure of *GaDamDet* Program
(Adapted from Lizskai, 2003)

The utility program, ModalFEM, simulates the measurement data and generates FRF input files for different finite element models. The user provides an input text file (*.inp) containing the finite element model of the structure. Using the input file, the utility program generates a binary MATLAB data file (*.mat) that contains simulated

measurement data for specific excitation and measurement locations and a specific imposed noise level.

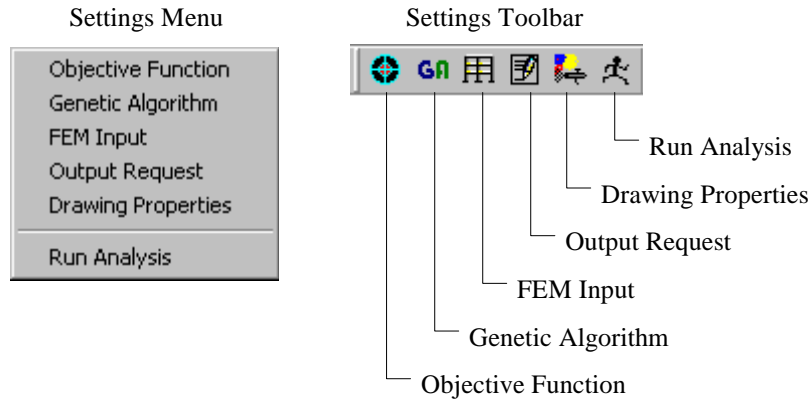


Figure 2.2 Settings Menu and Its Toolbar (Adapted from Lizskai, 2003)

The finite element model (FEM) input of the program opens a screen to let the user input two files:

1. Undamaged Finite Element Input File,
2. Matlab File containing measurement data.

The user is asked to input the undamaged finite element input card directly into the program. In comparison, the user prepares the damaged element input file and runs it in the utility program ModalFEM. The FEM input screen is shown in Figure 2.3.

ModalFEM provides the FRF of the defined damaged structure considering the location and severity of the damage provided by the damaged input file. Damage is imposed with a reduction in the stiffness for the desired element. This is done by reducing the Young Modulus of the damaged member by the percentage amount of the damage that is proposed. As stated before, all the information necessary to define the finite element model of any trial is stored in an input card. . The element numbers and

definitions (which ones are columns, beams or braces), dimensions and properties of these elements (Young Modulus, area, moment of inertia, Poisson's ratio, etc.), support conditions, etc. are defined with this input card. A sample input card with explanation of each parameter is provided in Appendix A.

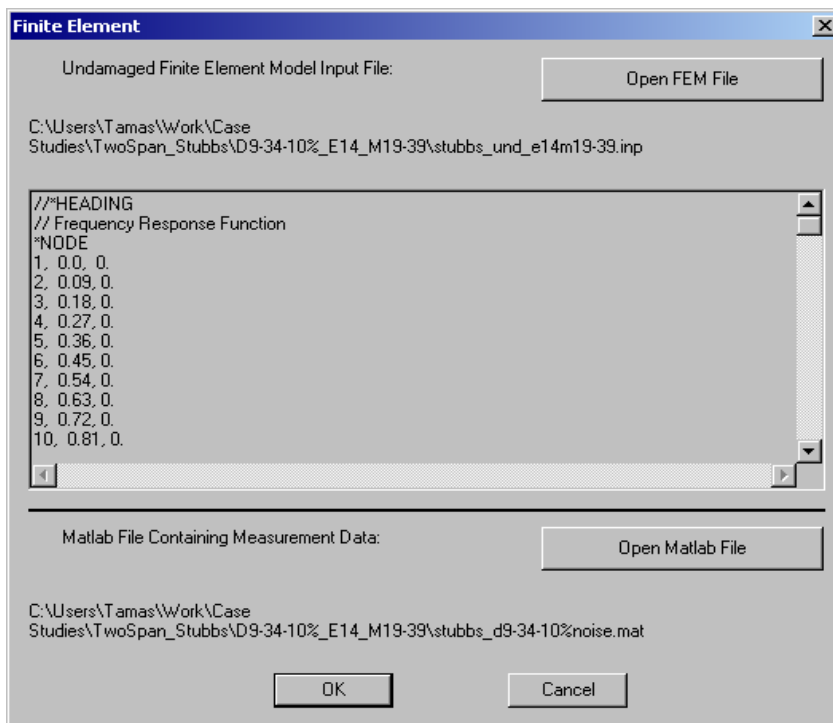


Figure 2.3 Finite Element Model Input and Matlab Measurement Data Files
(Adapted from Lizskai, 2003)

ModalFEM constructs the FRF measurements as MATLAB arrays. This MATLAB file is selected by the user in the FEM input screen as the damaged structure's input card, which is named as the "Matlab File Containing Measurement Data" in Figure 2.3.

Before running GaDamDet and performing structural damage detection, the user is able adjust any GA parameter, such as population size, crossover sides, coding type (binary or gray), mutation rate, variables (IRR or Fixed-Length), and set the optional process switches (Hillclimbing, Binary or Gray Coding, Elitism-on/off). The dialog box to input or change the genetic algorithm parameters is shown in Figure 2.4.

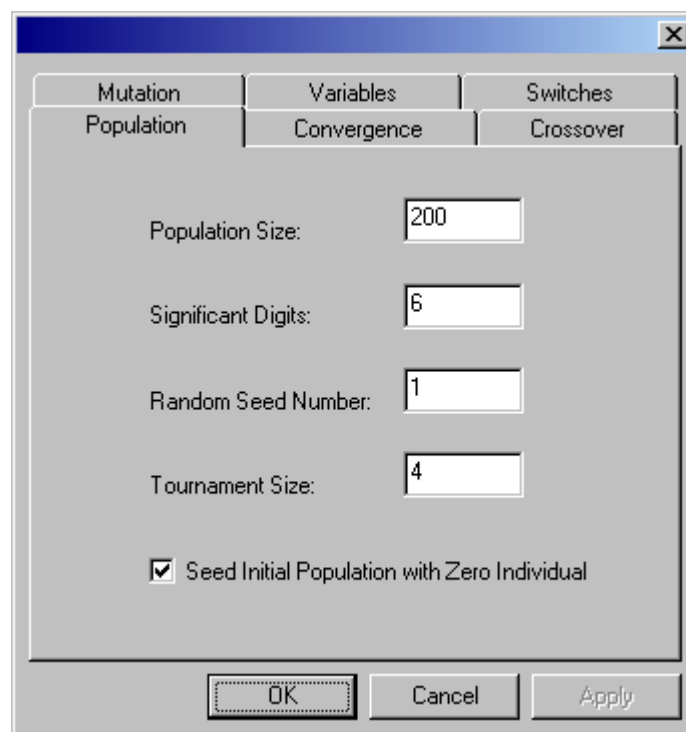


Figure 2.4 Genetic Algorithm Parameter Sheet
(Adapted from Lizskai, 2003)

The “Results” menu and its submenus offer two graphical output windows that show the genetic algorithm process results as either a “Structure Plot” or “Individual Plot”. The “Individual Plot” contains crucial information about the individual genetic

algorithm string encoding, including the fitness value, representation type, generation number, and number of gene instances. The “Structure Plot” shows the location of the damaged elements along with the damage severity directly on the structure by visually showing the two-dimensional structure and results. The severity of damage can be viewed by opening a small rectangular window showing the percent damage indicator when an element is highlighted with the cursor. The graphical output window of the “Structure Plot” menu is shown in Figure 2.5. The excitation and measurement locations and element numbers with corresponding damages (as a percentage) can be viewed in the output window.

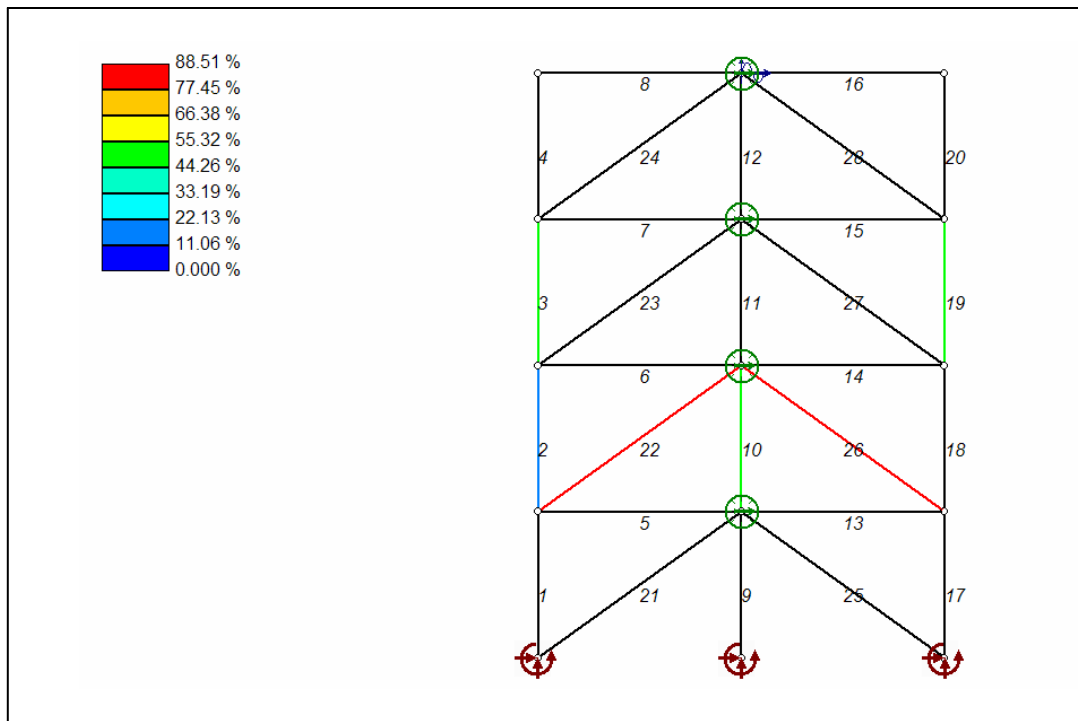


Figure 2.5 Structure Plot Option in GaDamDet

Before closing this section concerning the features of GaDamDet, a discussion of the “Hillclimbing” optimization option of the program is provided. Hillclimbing is an easy optimization method to implement as it only uses the information contained in the objective function to improve the current solution iteratively. Hillclimbing uses a single solution (point) during the search process. At each iteration, new solutions (points) are selected from the neighborhood of the current (best) solution. If the best among the newly selected points is better than the current point, then that solution becomes the current point and a new iteration starts. If there is no better point found among the new solutions, then another neighborhood is selected and tested. The process terminates if no further improvements are possible or another termination condition is satisfied, such as the number of iterations to be performed (Lizskai, 2003). The GA program employs the local hillclimber as described above in order to try to improve upon the solution obtained by the GA. The solution returned by the GA may be near-optimal due to the population converging or the GA process stopping because the maximum number of generations is exceeded. The local hillclimber is often effective in improving the GA solution toward the global optimum. The performance of the hillclimber in this research is discussed in the Results and Discussions (Section 5).

2.2 Description of the Experimental Response Measurement Program Datagen

Datagen is a Matlab program developed during Phase I of the IASC-ASCE benchmark problem. Datagen can be used to simulate the dynamic response of the 3-D four-story, two-bay by two-bay steel UBC Test Structure under various damage cases. The first version of Datagen (called Datagen version 1999.08.28) was developed on 28-August-1999 after a meeting of the ASCE Task Group on Structural Health Monitoring at California Institute of Technology. After that, the program was continuously updated according to the requirements of the ASCE task group.

The Datagen user is able to select any of the 6 damage scenarios defined officially as part of the benchmark problem using the dialog boxes that appear after

running the program in Matlab environment. A user-defined damage case can also be specified in Datagen that allows the user to specify any member or members as damaged, which allows other damage cases to be investigated. Simulated noise can also be introduced to the measurements obtained. The dialog box used to input damage scenarios is shown in Figure 2.6. A reference undamaged case is also available in order to simulate the behavior of the undamaged structure.

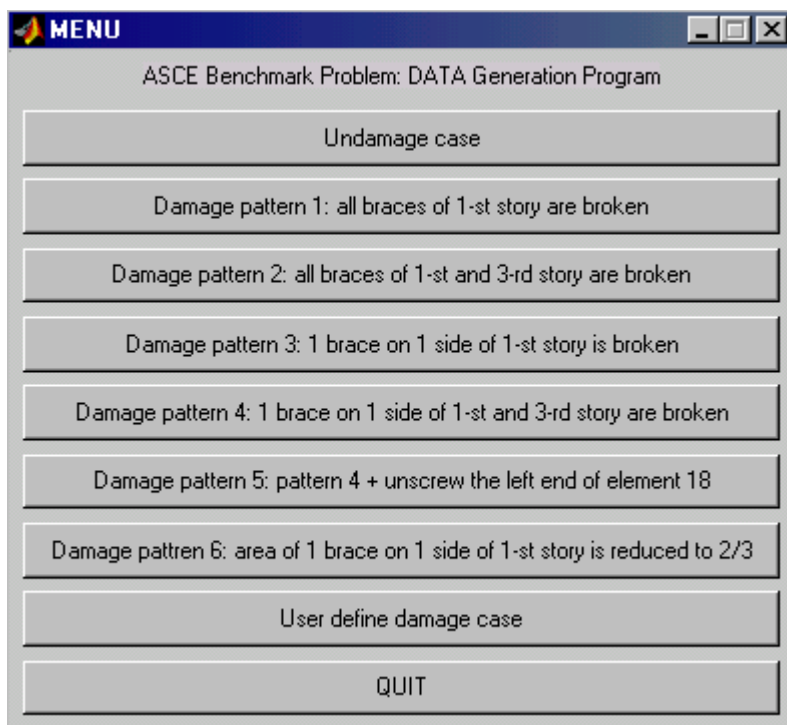


Figure 2.6 Damage Cases Defined by Datagen for the UBC Benchmark Problem

The program determines the forcing function and corresponding acceleration measurements for two main cases. These are forcing vectors in the y direction on each floor or in the x and y directions at the roof, with the option of using either 12 or 120

DOF model. The 12 DOF model is a shear-building model that constrains all DOFs except for two translations and one rotation per floor. The 120 DOF model only requires the floor nodes to have same horizontal translation and in-plane rotation. This model is used to simulate the response measurements, while the model used in the identification analyses remains simpler (12 DOF). The horizontal slab panels are assumed to contribute only towards in-plane stiffness making the floor behave as a rigid plate with respect to in-plane motions only. The remaining out of plane degrees of freedoms (vertical motion, pitching/rolling of the floor) are active. The columns and beams are modeled as Euler Bernoulli beams in both the 12 and 120 DOF finite element models. The braces are modeled as bars with no bending stiffness. Different case numbers are given to each combination of model and load in the program which can be seen in Figure 2.7.

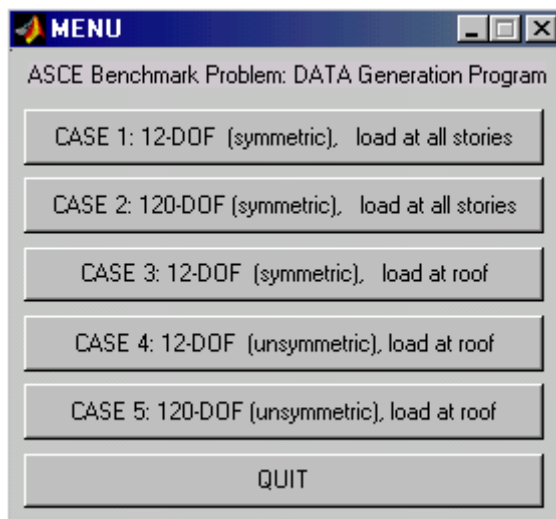
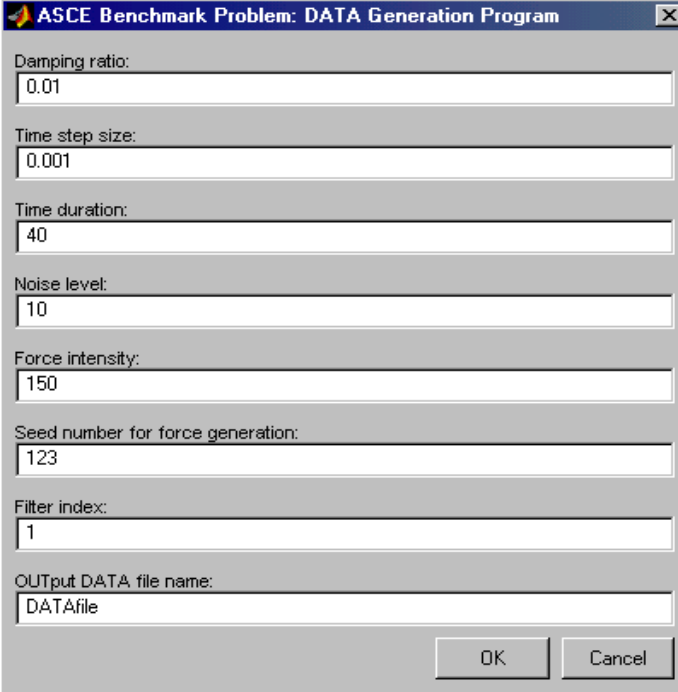


Figure 2.7 Datagen Case IDs

Datagen allows the user to adjust the set of model parameters, including the damping ratio, time duration and step size, noise level, and force intensity. The parameter sheet to input these parameters can be seen in Figure 2.8. The list of all input and output parameters as well as the files in Datagen Package are given in Appendix B.



The image shows a dialog box titled "ASCE Benchmark Problem: DATA Generation Program". It contains several input fields for parameters:

- Damping ratio: 0.01
- Time step size: 0.001
- Time duration: 40
- Noise level: 10
- Force intensity: 150
- Seed number for force generation: 123
- Filter index: 1
- OUTPUT DATA file name: DATAfile

At the bottom right, there are "OK" and "Cancel" buttons.

Figure 2.8 Datagen Parameter Sheet

2.2.1 Definition of UBC Test Structure:

The Benchmark Structure was built in one-third scale at the University of British Columbia. It is a two-bay by two-bay, four-story, rectangular steel structure, which is 3.6 m tall and 2.5 m wide. Each bay is 1.25 m x 0.9 m. Hot rolled B100 x 9 members are used for the columns, and S75 x 11 members are used for the floor beams. L25 x 25 x 3

sections are used for the bracing members on each floor. There is one floor slab per bay on each floor: four 800 kg slabs at the first floor, four 600 kg slabs at the second and third floor and four 400 kg slabs at the fourth floor. In order to simulate an asymmetric mass distribution, one of the 400 kg slabs is replaced with a 550 kg one in Cases 4 and 5 of the benchmark problem. UBC Test Structure is shown in Figure 2.9, while section properties can be seen in Table 2.1. This photograph was taken by the participants of the benchmark problem during the experimental stage (Phase II) and is taken directly from the IASC-ASCE SHM Task Group website (<http://wusceel.cive.wustl.edu/asce.shm>).



Figure 2.9 UBC Test Structure
(Adapted from the IASC-ASCE SHM Task Group Web Site)

Table 2.1 The Section Properties of the Benchmark Structure

Property	Columns	Beams	Braces
Section Type	B x 100 x 9	S x 75 x 11	1.25 x 25 x 3
Cross Sectional Area [m ²]	1.133 x 10 ⁻³	1.43 x 10 ⁻³	0.141 x 10 ⁻³
Moment of Inertia (Strong) [m ⁴]	1.97 x 10 ⁻⁶	1.22 x 10 ⁻⁶	0
Moment of Inertia (Weak) [m ⁴]	0.664 x 10 ⁻⁶	0.249 x 10 ⁻⁶	0
St. Ven. Torsion Constant [m ⁴]	8.01 x 10 ⁻⁹	38.2 x 10 ⁻⁹	0
Young's Modulus [Pa]	2 x 10 ¹¹	2 x 10 ¹¹	2 x 10 ¹¹
Mass per unit length [kg/m]	8.89	11.0	1.11

2.3 Discussion of the Hybrid Structural Damage Identification Method Proposed

In Cases 1 and 2 of ASCE benchmark problem, the structure's 3-D response is measured under ambient vibration, while in Cases 3, 4 and 5, the structure's response to a diagonally placed shaker is simulated. These models are analyzed as multiple input/multiple output and single input/multiple output problems, respectively. The input to the system is a forcing function vector in the x or y direction and the output from the system is 16 acceleration measurements. In comparison, the SDIM provided by GaDamDet uses a 2-D model (one of the perimeter frames can be chosen), which allows only 4 of these acceleration records to be used. For all the trials performed, four of the FRF s in either the weak - y or strong - x direction are computed, which corresponds to a FRF at each floor level for the 2-D frame modeled.

Instead of using the utility program ModalFEM to simulate the damaged structure's FRFs as was done in the previous research effort, the results of the ASCE Benchmark problem are used to provide the information required for the damaged structure input card by GaDamDet. In the simplest terms, the utility program ModalFEM, is replaced with the simulated results obtained from the first phase of the ASCE benchmark problem. The SDIM provided by GaDamDet changes the stiffness values of the baseline (undamaged) structural model until the differences between the

measured responses provided by Datagen and those predicted by the undated baseline model are minimized. The stiffness values in the updated model found by GaDamDet can be used to identify the severity and the location of the damage. This hybrid procedure will provide the capability to identify damage in more realistic structures since the measurement information of the damaged structure is collected experimentally from the complete three-dimensional structure and the FRFs can be easily calculated using a simple data processing algorithm, which will be defined in Section 3. The program assumes that a finite element model of the intact structure is present. However, it does not require having any records taken from the undamaged structure which may not be available most of the time. Thus, by leaving ModalFEM out, measurement information for a structure without any indication of damage location or quantity is collected, which is the case of all real-world applications.

2.3.1 Modifications Required in the Finite Element Model Used by GaDamDet

Processing the measurement information data obtained from Datagen, however, is not the only procedure required in replacing the utility program ModalFEM. Since a finite element model of the structure must be available for the SDIM to work, the model has to be defined that reflects the behavior of the structure defined in the benchmark experiment as accurately as possible. This is a challenging process, since the simulated model of the UBC structure is a 3-D model with slab elements defined at each floor, while the input card used to construct the finite element models in GaDamDet can only build simpler 2-D frame models. The difficulty with this reduction in the dimensions of the models is that the dynamic behavior of the real structure is dominated by the floor slabs due to their large mass compared to other structural elements and due to the lateral stiffness the slabs add to each floor. To overcome this problem, the weight of the slabs is computed using the *DENSITY card in order to create the 2-D model of the structure. In addition the total weight of the structure is loaded to one perimeter frame only.

The masses distributed to the floors are:

1st floor: 4 – 800 kg slabs

2nd floor: 4 – 600 kg slabs

3rd floor: 4 – 600 kg slabs

4th floor: 4 – 400 kg slabs

The volume of a beam is calculated:

$$\text{Volume} = (1.43 \times 10^{-3}) \cdot (1.25) = 0.0017875 \text{ m}^3 \quad (2.8)$$

The modified density of each beam at each floor can be defined as:

$$D1 = \frac{\text{Mass}}{\text{Volume}} = \frac{1600}{0.0017875} = 895106 \text{ kg/m}^3 \quad (2.9)$$

$$D2 = \frac{\text{Mass}}{\text{Volume}} = \frac{1200}{0.0017875} = 671328 \text{ kg/m}^3 \quad (2.10)$$

$$D3 = \frac{\text{Mass}}{\text{Volume}} = \frac{800}{0.0017875} = 447552 \text{ kg/m}^3 \quad (2.11)$$

The density of the steel (7500 kg/m^3) is kept for defining the columns and braces in the structure. The damping ratio is set at 0.01 for the first four modes and then increased to 0.015 for the other modes extracted, which is typically 4 modes. The moment of inertia of the beams is doubled to $2.44 \times 10^{-6} \text{ m}^4$ in order to simulate the same rigid effect in the 2-D structural frame as they provide in the real 3-D structure. Columns have the same moment of inertia in both models, which is $1.97 \times 10^{-6} \text{ m}^4$ in the strong and $0.664 \times 10^{-6} \text{ m}^4$ in the weak directions.

2.3.2 *Modifications Required in the Measurement / Excitation Pairs*

The number of FRF measurements used depends on the number of available measurement/excitation pairs. Ideally, one should obtain an FRF matrix that has a size equal to the product of number of measurements and number of excitations. For example with four measurements and four excitations, sixteen different FRFs should be obtained as a function of frequency. However, ModalFEM only takes the number of measurements into account when FRFs are calculated, which means it assumes a single excitation force. As an example, the following input card will produce an FRF matrix with four arrays. (Each of the array columns is a function of frequency)

```
*NSET, NSET=MEAS
    21, 24, 27, 30
*NSET, NSET=EXC
    42
```

The calculated FRFs should relate the excitation with each of the measurements obtained from imposing the excitation. Thus, EXC 1- MEAS 1 (42-21) , EXC 1- MEAS 2 (42-24), EXC 1- MEAS 3 (42-27), EXC 1- MEAS 4 (42-30) is the set of excitation/measurement pairs for this set of FRFs. It should be noted that the FRF measurements are obtained by inverting the dynamic stiffness in ModalFEM instead of processing the excitation/measurement pairs. However, this kind of a logical argument is defined in order to understand the information provided by the program algorithm. Furthermore, the same process will need to be applied with in order to obtain the damaged structures' FRFs from simulated data later on.

Using a different input card produces the following results:

*NSET, NSET=MEAS

21, 24, 27, 30

*NSET, NSET=EXC

42, 45, 48, 51

Sixteen FRFs are expected in this type of an input. However an FRF matrix with 4 arrays is obtained using ModalFEM and each excitation is related with its corresponding measurement in the program. Thus, EXC 1- MEAS 1 (42-21), EXC 2- MEAS 2 (45-24), EXC 3- MEAS 3 (48-27), EXC 4- MEAS 4 (51-30) is the set of excitation/measurement pairs for this set of FRFs. This can easily be proved if one tries to obtain excitation/measurement pairs by inputting the excitations one by one instead of applying them all simultaneously.

Thirteen different trials were run using a simple cantilever beam to prove this algorithm. The results obtained above were supported and the same technique will be used throughout the research in order to obtain the FRF measurements.

2.3.3 *Required Input/Output Parameters in Datagen:*

There are two cases that will be considered for the simulated stage of the experiment.

1. Force input (in y direction at each floor) / acceleration output (in x and y direction at each floor).
2. Force input (in x and y direction at the roof) / acceleration output (in x and y direction at each floor.)

In both cases, the system appears to be a multiple input/multiple output model; although it will be proved that the second case should be analyzed as a single input/multiple output case later in this thesis.

Since GaDamDet uses a 2-D model of the system currently, one of the four perimeter frames is chosen for analysis. Because of this feature, only four of the sixteen acceleration measurements will be used as the output parameters in the first case. Four inputs are applied to the edge columns and four outputs are taken from the middle columns (all in y direction). Input/output parameters and their locations for the first case can be seen in Figure 2.10. Only the four acceleration measurements taken weak direction are shown for simplicity. These are the records that will be used in frequency response function calculations in the following sections. The second case defines two inputs and sixteen outputs. The two inputs are at the roof level in the x and y directions while outputs are taken from the middle columns in y direction like the first case. Figure 2.11 shows the input/output parameters and locations both in weak and strong directions.

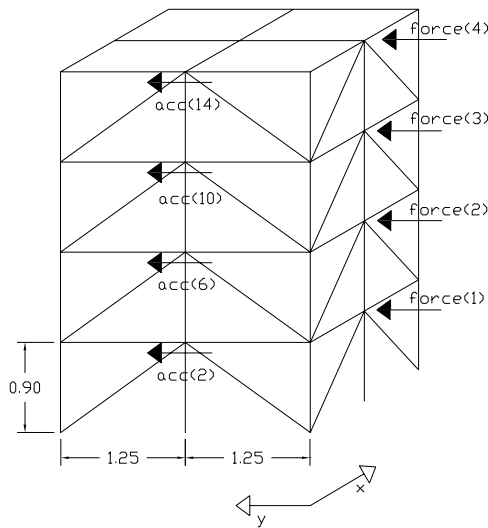


Figure 2.10 Input/Output Parameters for the Multiple-Input/Multiple-Output Model (Only in Weak Direction)

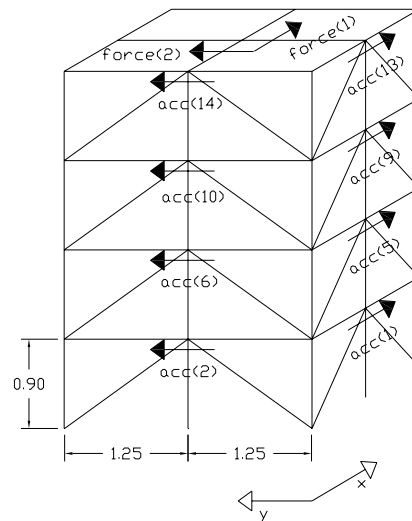


Figure 2.11 Input/Output Parameters for the Single-Input/Multiple-Output Model (Both in Weak and Strong Direction)

Only four acceleration records in each direction are shown for simplicity. The second case actually simulates a diagonally placed shaker's responses on the structure.

For the first case, the excitations applied at each floor in weak (y) direction are designed as Gaussian white noise (Gaussian white noise processes passed through a 6th order low-pass Butterworth filter with a 100-Hz cutoff). The accelerometers return noisy sensor measurements where noise is defined as Gaussian pulse processes with RMS %10 of the RMS of the roof acceleration. The data generation uses a discrete-time integration at 1 KHz and provides the sensor measurements at 1 KHz with an option of user defined lower sampling rates. The first case was actually designed to simulate the response of the structure to ambient vibration (wind loading at each floor in y-direction), but in order to simulate a process like this, a forcing function must be defined. The second case simulates a diagonally placed shaker's responses. The force in the shaker is also designed as a Gaussian white noise process filtered with a low-pass Butterworth filter.

3 FREQUENCY RESPONSE FUNCTIONS

This section discusses how frequency response functions (FRF) can be obtained from random measurement data. The input/output models examined include single input/single output, single input/multiple output, and multiple input/output relationships. After defining the basic concepts, the section discusses the mathematical formulations of the FRFs for each type of model. A simple algorithm is then introduced that can determine FRFs for different input/output measurement response problems. All definitions, concepts and equations as well as figures are based on “Random Data Analysis and Measurement Procedures (2000)” and “Engineering Applications of Correlation and Spectral Analysis (1980)” by Julius S. Bendat and Allan G. Piersol.

3.1 Random Data

A physical phenomenon, along with the data representing it, is considered random when a future time history record from an experiment cannot be predicted within a reasonable experimental error. Each observation of the phenomenon will be unique and, therefore, cannot be described by an explicit mathematical relationship. A single time history representing a random phenomenon is called a sample function, whereas the collection of all possible sample functions that the random phenomenon might have produced is called a random process or a stochastic process. Random data can be classified in two main categories; stationary or non-stationary. Stationary random data may further be categorized as being either ergodic or nonergodic.

In this research, the records obtained from the first phase of the benchmark structure test problem are stationary. Therefore, all the formulations for FRFs discussed in this research are valid for stationary random data.

3.1.1 Stationary Random Data

When a physical phenomenon is considered in terms of a random process, the properties of the phenomenon can hypothetically be described at any instant of time by computing average values over the collection of sample functions that describe the random process. The mean value (first moment) of the random process at some time t_1 can be computed by taking the instantaneous value of each sample function of the ensemble (collection of sample functions) at time t_1 , summing the values, and dividing by the number of sample functions. In a similar manner, a correlation (joint moment) between the values of the random process at two different times (called the autocorrelation function) can be computed by taking the ensemble average of the product of instantaneous values at two times, t_1 and $t_1 + \tau$. Thus, for the random process $\{x(t)\}$, where the symbol $\{ \}$ is used to denote an ensemble of sample functions, the mean value $\mu_x(t_1)$ and the autocorrelation function $R_{xx}(t_1, t_1 + \tau)$ are given by

$$\mu_x(t_1) = \lim_{N \rightarrow \infty} \frac{1}{N} \sum_{k=1}^N x_k(t_1) \quad (3.1)$$

$$R_{xx}(t_1, t_1 + \tau) = \lim_{N \rightarrow \infty} \frac{1}{N} \sum_{k=1}^N x_k(t_1) x_k(t_1 + \tau) \quad (3.2)$$

where the final summation assumes each sample function is equally likely.

For the general case where $\mu_x(t_1)$ and $R_{xx}(t_1, t_1 + \tau)$ defined in equations (3.1) and (3.2) vary as time t_1 varies, the random process $\{x(t)\}$ is said to be non-stationary. For the special case where $\mu_x(t_1)$ and $R_{xx}(t_1, t_1 + \tau)$ do not vary as time t_1 varies, the random process $\{x(t)\}$ is said to be weakly stationary or stationary in wide sense. For a weakly stationary random process, the mean value is constant and the autocorrelation function is dependent only on the time displacement τ . This means that $\mu_x(t_1) = \mu_x$ and $R_{xx}(t_1, t_1 + \tau) = R_{xx}(\tau)$.

For the special case where all possible moments and joint moments are time invariant, the random process $\{x(t)\}$ is said to be strongly stationary.

3.1.1.1 Ergodic Stationary Random Data

For almost all stationary data, the average values computed over the ensemble at time t_1 will equal the corresponding average values computed over time from a single time history record. If the k^{th} sample function of the random process is considered, then the mean value $\mu_x(k)$ and the autocorrelation function $R_{xx}(\tau, k)$ of the function are given by

$$\mu_x(k) = \lim_{T \rightarrow \infty} \frac{1}{T} \int_0^T x_k(t) dt \quad (3.3)$$

$$R_{xx}(\tau, k) = \lim_{T \rightarrow \infty} \frac{1}{T} \int_0^T x_k(t) x_k(t + \tau) dt \quad (3.4)$$

If the random process $\{x(t)\}$ is stationary, and $\mu_x(k)$ and $R_{xx}(\tau, k)$ defined in equations (3.3) and (3.4) do not differ when computed over different sample functions, the random process is said to be ergodic. That is, $\mu_x(k) = \mu_x$ and $R_{xx}(\tau, k) = R_{xx}(\tau)$. Only random processes can be ergodic. All properties of ergodic random processes can be determined by performing time averages over a single sample function. For this reason, the properties of stationary random phenomena can be measured properly from a single observed time history record. In practice, random data representing stationary physical phenomena are generally ergodic.

3.2 Analysis of Random Data

It was stated in the Section 3.1 that random data can not be represented by an explicit mathematical equation. Thus, a statistical procedure must be used to define the

descriptive properties of the data. Bendat and Piersol defined the basic statistical properties for describing single stationary random records as the following:

1. Mean and mean square values
2. Probability density functions
3. Autocorrelation functions
4. Autospectral density functions

The mean value $\mu_x(k)$ and the variance σ_x^2 for a stationary record represent the central tendency and dispersion, respectively, of the data. The mean square value ψ_x^2 , which equals the variance plus the square of the mean, provides a measure of the combined central tendency and dispersion. The mean value is estimated by simply computing the average of all data values in the record. The mean square value is similarly estimated by computing the average of all squared data values. By first subtracting the mean value estimate from all the data values, the mean square value computation yields a variance estimate.

The probability density function $p(x)$ for a stationary record represents the rate of change of probability with data value. The function $p(x)$ is generally estimated by computing the probability that the instantaneous value of the single record will be in a particular narrow amplitude range centered at various data values, and then dividing by the amplitude range. The total area under the probability density function over all data values will be unity. This indicates the certainty of the fact the data values fall between $-\infty$ and $+\infty$. The partial area under the probability density function from $-\infty$ to some given value x represents the probability distribution function, $P(x)$. The area under the probability density function between any two values x_1 and x_2 is given by $P(x_2) - P(x_1)$. This area defines the probability that any future data values at a randomly selected time will fall within this amplitude interval.

The autocorrelation function $R_{xx}(\tau)$ for a stationary record is a measure of time-related properties in the data that are separated by fixed time delays. The level of autocorrelation can be estimated by delaying the record relative to itself by some fixed

time delay τ , and then multiplying the original record by the delayed record and taking the average of the resulting product values over the available record length or over some desired portion of this record length. The procedure is repeated for all time delays of interest.

The autospectral (also called power spectral) density function $G_{xx}(f)$ for a stationary record represents the rate of change of the mean square value with respect to frequency. This measure is estimated by computing the mean square value in a narrow frequency band at various center frequencies, and then dividing by the frequency band. The total area under the autospectral density function over all frequencies will be the total mean square value of the record. The partial area under the autospectral density function from f_1 to f_2 represents the mean square value of the record associated with that frequency range.

For pairs of random records taken from two different stationary random processes, there are several joint statistical properties of importance and can be stated as the following:

1. Joint probability density functions
2. Cross-correlation functions
3. Cross-spectral density functions
4. Frequency response functions
5. Coherence functions

The first three functions measure fundamental properties shared by the pair of records in the amplitude, time, or frequency domains. From knowledge of the cross-spectral density function between the pair of records, as well as their individual autospectral density functions, one can compute theoretical linear response functions (gain factors and phase factors) between the two records. The coherence function is a measure of the accuracy of the assumed linear input/output model, and can be computed from the measured autospectral and cross-spectral density functions.

3.3 Input/Output Relations

Input/output cases of common interest can usually be considered as combinations of one or more of the following linear system models:

1. Single-input/single-output model
2. Single-input/multiple-output model
3. Multiple-input/single-output model
4. Multiple-input/multiple-output model

In all cases, there may be one or more parallel transmission paths with different time delays between each input point and output point. For the multiple input cases, the various inputs may or may not be correlated with each other.

For a single-input/single-output model, $x(t)$ and $y(t)$ are the measured input and output stationary random records, and $n(t)$ is the unmeasured extraneous output noise. The quantity $H_{xy}(f)$ is the frequency response function of a constant-parameter linear system $x(t)$ and $y(t)$. This simple system is shown in Figure 3.1.

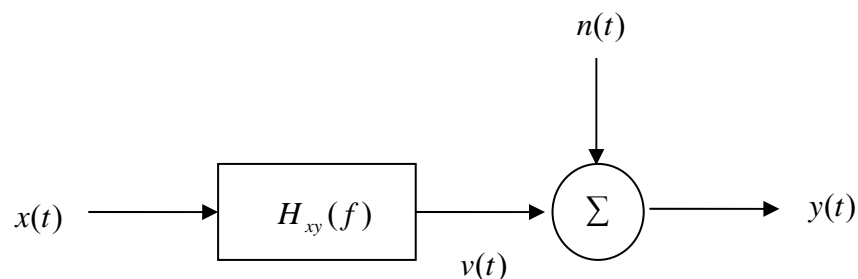


Figure 3.1 Single-Input/Single-Output System with Output Noise
(Adapted from Bendat/Piersol, 2000)

As an extension of this system, a single-input/ multiple-output model is shown in Figure 3.2. The frequency response function (FRF) $H_{xi}(f)$ is defined as the constant-parameter linear system between the input $x(t)$ and the output $y_i(t)$. There are as many frequency response functions as the number of outputs in the system in the multiple output case. The noise terms $n_i(t)$ represent unmeasured extraneous output noise at the different output measurement points.

Single-input models can be solved using measured autospectral and cross-spectral density functions. Multiple-input/multiple-output models are analyzed using two different techniques derived from an extension of the simple single-input case.

3.4 Basic Dynamic Characteristics

Before finishing the discussion of the basic concepts, several fundamental definitions related to the dynamic behavior of physical systems will be summarized. An ideal system has constant parameters, is stable, and is linear between two clearly defined points called the input or excitation and the output or response point. A simple has constant parameters if all fundamental properties of the system are time invariant. A linear system is one in which the response characteristics of the system are additive and homogenous.

The term *additive* means that the output to a sum of units is equal to the sum of the outputs produced by each input individually. The term *homogenous* means that the output produced by a constant times the input is equal to the constant times the output produced by the input alone. If x represents the input and $f(x)$ represents the output, then the system is said to be linear if for any two inputs x_1, x_2 , and a constant c satisfies the following:

$$f(x_1 + x_2) = f(x_1) + f(x_2) \quad \text{additive property} \quad (3.5)$$

$$f(cx) = cf(x) \quad \text{homogeneous property} \quad (3.6)$$

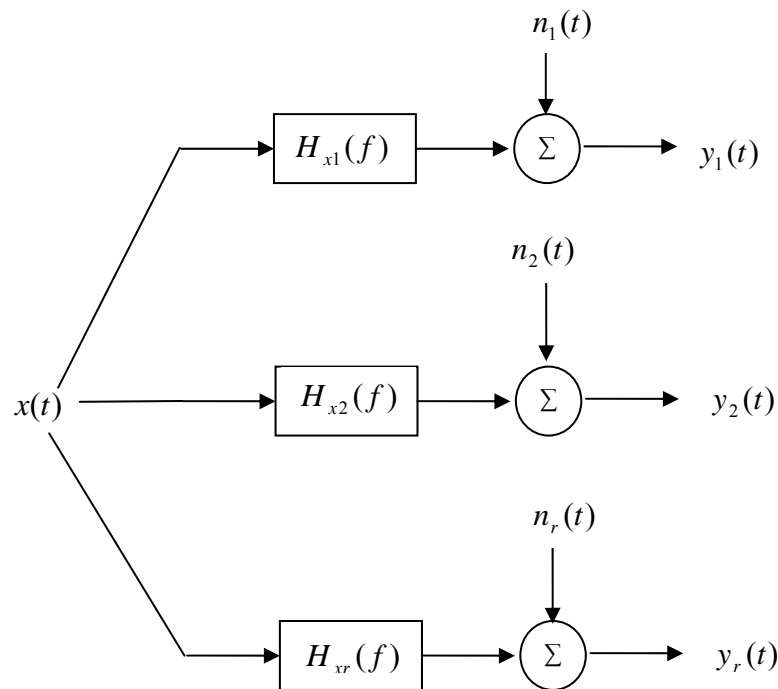


Figure 3.2 Single-Input/Multiple-Output System with Output Noise
(Adapted from Bendat/Piersol, 2000)

The response characteristics for many physical systems may be assumed to be linear over at least a limited range of inputs without involving any unreasonable errors.

The dynamic characteristics of a constant-parameter linear system can be described by an impulse response function $h(\tau)$, also called the weighting function, which is defined as the output of the system at any time to a unit impulse input applied a

time τ before. For any arbitrary input $x(t)$, the system output $y(t)$ is given by the *superposition or convolution integral*:

$$y(t) = \int_{-\infty}^{\infty} h(\tau)x(t-\tau)d\tau \quad (3.7)$$

In order for a constant-parameter linear system to be physically realizable (causal), it is necessary that the system respond only to past inputs. Therefore the following constraint must be satisfied,

$$h(\tau) = 0 \quad \text{for } \tau < 0 \quad (3.8)$$

For physical systems, the effective lower limit of the integration in Equation (3.7) is zero other than negative infinity ($-\infty$).

A constant-parameter linear system is said to be stable if every possible bounded input function produces a bounded output function. Thus, from Equation (3.7):

$$|y(t)| = \left| \int_{-\infty}^{\infty} h(\tau)x(t-\tau)d\tau \right| \leq \int_{-\infty}^{\infty} |h(\tau)||x(t-\tau)|d\tau \quad (3.9)$$

When the input $x(t)$ is bounded, there exists some finite constant A such that

$$|x(t)| \leq A \quad \text{for all } t \quad (3.10)$$

Hence from Equation (3.9)

$$|y(t)| \leq A \int_{-\infty}^{\infty} |h(\tau)|d\tau \quad (3.11)$$

Thus if the constant-parameter linear weighting function $h(\tau)$ is absolutely integrable,

$$\int_{-\infty}^{\infty} |h(\tau)| d\tau < \infty \quad (3.12)$$

then the output will be bounded and the system is stable.

3.5 Frequency Response Functions

If a constant-parameter linear system is physically realizable and stable, then the dynamic characteristics of the system can be described by a *frequency response function* $H(f)$, which is defined as the Fourier transform of weighting function $h(\tau)$.

$$H(f) = \int_0^{\infty} h(\tau) e^{-j2\pi f\tau} d\tau \quad (3.13)$$

In constant-parameter linear systems, if Fourier transform of both sides of Equation (3.7) is taken, then an important relationship is obtained:

$$Y(f) = H(f)X(f) \quad (3.14)$$

where, $X(f)$ is the Fourier transform of an input $x(t)$ and $Y(f)$ is the Fourier transform of the resulting output $y(t)$. This equation assumes that these forms exist.

The frequency response function (FRF) is generally a complex-valued quantity that may be thought of in terms of a magnitude and a phase angle. If $H(f)$ is written in complex polar notation, then the following equation is obtained.

$$H(f) = |H(f)|e^{-j\phi(f)} \quad (3.15)$$

where, the absolute value $|H(f)|$ is called the system gain factor, and the phase angle $\phi(f)$ is called the system phase factor.

A FRF is a function of only frequency in a constant-parameter linear system. If the system is nonlinear, then $H(f)$ will also be a function of the applied input (excitation). If the parameters of the system are not constant, $H(f)$ will also be a function of time.

3.6 Single-Input/Output Relationships

The theory and formulations of input/output relationships for single-output problems are discussed in this section using the concepts defined in “Random Data Analysis and Measurement Procedures (2000)” by Bendat and Piersol. It is assumed that the records involved are obtained from stationary random process with zero mean values and that the system is a constant-parameter linear system.

3.6.1 Single-Input/Single-Output Models

Consider a constant-parameter linear system with a weighting function $h(\tau)$ and frequency response function $H(f)$ that is subjected to a well-defined single input $x(t)$ from a stationary random process $\{x(t)\}$, which produces a well-defined output $y(t)$.

Under ideal conditions, the output $y(t)$ is given by the convolution integral defined in Equation (3.7) with its boundaries switched to zero to positive infinity.

$$y(t) = \int_0^{\infty} h(\tau)x(t-\tau)d\tau \quad (3.16)$$

where $h(t) = 0$ for $\tau < 0$ when the system is physically realizable. The product $y(t)y(t + \tau)$ is given by

$$y(t)y(t + \tau) = \int_0^{\infty} \int_0^{\infty} h(\alpha)h(\beta)x(t - \beta)x(t + \tau - \alpha)d\alpha d\beta \quad (3.17)$$

Taking the expected values of both sides yields the *input/output autocorrelation* relation.

$$R_{yy}(\tau) = \int_0^{\infty} \int_0^{\infty} h(\alpha)h(\beta)R_{xx}(\tau + \beta - \alpha)d\alpha d\beta \quad (3.18)$$

Similarly, the product $x(t)y(t + \tau)$ is given by

$$x(t)y(t + \tau) = \int_0^{\infty} h(\alpha)x(t)x(t + \tau - \alpha)d\alpha \quad (3.19)$$

Taking the expected values of both sides yields the *input/output cross-correlation* relation.

$$R_{xy}(\tau) = \int_0^{\infty} h(\alpha)R_{xx}(\tau - \alpha)d\alpha \quad (3.20)$$

Equation (3.20) is a convolution integral of the same form as Equation (3.16).

Taking the direct Fourier transforms of Equations (3.18) and (3.20) after various algebraic steps yields the set of two-sided spectral density functions $S_{yy}(f)$, $S_{xx}(f)$ and $S_{xy}(f)$.

$$S_{xx}(f) = \int_{-\infty}^{\infty} R_{xx}(\tau) e^{-j2\pi f\tau} d\tau \quad (3.21)$$

$$S_{yy}(f) = \int_{-\infty}^{\infty} R_{yy}(\tau) e^{-j2\pi f\tau} d\tau \quad (3.22)$$

$$S_{xy}(f) = \int_{-\infty}^{\infty} R_{xy}(\tau) e^{-j2\pi f\tau} d\tau \quad (3.23)$$

where Equation (3.23) is called the *cross-spectral density function*, or simply *cross-spectrum* between $x(t)$ and $y(t)$. Equation (3.21) and (3.22) are called *autospectral density functions of $\{x_k(t)\}$ and $\{y_k(t)\}$* (which are often called as *autospectrum* or sometimes the *power spectral density functions*). Spectral density functions satisfy the following important formulas

$$S_{yy}(f) = |H(f)|^2 S_{xx}(f) \quad (3.24)$$

$$S_{xy}(f) = H(f) S_{xx}(f) \quad (3.25)$$

Equation (3.24) is called the *input/output autospectrum relation*, while Equation (3.25) is called the *input/output cross-spectrum relation*. Equation (3.24) is a real-valued relation containing only the gain factor $|H(f)|$ of the system. Equation (3.25) is a complex-valued relation, which can be broken down into a pair of equations to give both the gain factor $|H(f)|$ and the phase factor $\phi(f)$ of the system.

The given equations apply only to ideal situations where no extraneous noise exists at input or output points, and the systems must have no time-varying or nonlinear characteristics.

In terms of one-sided spectral density functions $G_{xx}(f)$, $G_{yy}(f)$ and $G_{xy}(f)$, where $G(f) = 2S(f)$ for $f > 0$, Equations (3.24) and (3.25) becomes

$$G_{yy}(f) = |H(f)|^2 G_{xx}(f) \quad (3.26)$$

$$G_{xy}(f) = H(f)G_{xx}(f) \quad (3.27)$$

An alternative direct transform is available to derive Equations (3.26) and (3.27) without first computing the correlation expressions of Equations (3.18) and (3.20). For any pair of long but finite records of length T, Equation (3.16) is equivalent to Equation (3.14). Using Equation (3.14), the following expression can be obtained:

$$Y^*(f) = H^*(f)X^*(f) \quad (3.28)$$

where, [*] denotes complex conjugates of the expressions. It follows that,

$$|Y(f)|^2 = |H(f)|^2 |X(f)|^2 \quad (3.29)$$

$$X^*(f)Y(f) = H(f)|X(f)|^2 \quad (3.30)$$

By taking the expectation of the last two equations over different independent records, multiplying by (2/T), and letting T increase without bound yields the same equations as Equation (3.26) and (3.27). Using these expressions, the frequency response function, $H(f)$ can be calculated:

$$H(f) = \frac{G_{xy}(f)}{G_{xx}(f)} \quad (3.31)$$

Another formula for $H(f)$ can be obtained by considering the complex conjugation of Equation (3.27).

$$G_{xy}^*(f) = G_{yx}(f) = H^*(f)G_{xx}(f) \quad (3.32)$$

where

$$G_{yx}(f) = |G_{xy}(f)|e^{j\phi_{xy}(f)} \quad (3.33)$$

$$H^*(f) = |H(f)|e^{j\phi(f)} \quad (3.34)$$

To determine the phase factor of the system, the following formula can be used

$$\frac{G_{xy}(f)}{G_{yx}(f)} = \frac{H(f)}{H^*(f)} = e^{-j2\phi(f)} \quad (3.35)$$

Using Equations (3.26) and (3.32), the complete FRF of the system, can be obtained as:

$$G_{yy}(f) = H(f)[H^*(f)G_{xx}(f)] = H(f)G_{yx}(f) \quad (3.36)$$

Thus, the frequency response function can be obtained as:

$$H(f) = \frac{G_{yy}(f)}{G_{yx}(f)} \quad (3.37)$$

Equation (3.37) will give the same FRF functions as (3.31) in ideal situations (noise free environment and infinite number of measurements).

Assuming $G_{xx}(f)$ and $G_{yy}(f)$ are both different from zero, the coherence function between the input $x(t)$ and the output $y(t)$ can be defined as:

$$\gamma^2_{xy}(f) = \frac{|G_{xy}(f)|^2}{G_{xx}(f)G_{yy}(f)} \quad (3.38)$$

The ordinary coherence function is a real-valued quantity that satisfies the following equation for all f .

$$0 \leq \gamma^2_{xy}(f) \leq 1 \quad (3.39)$$

For the ideal case of a constant-parameter linear system with a single clearly defined input and output, the coherence function will be unity. If the input and output are completely unrelated, then the coherence function will be zero. Having a coherence function value other than zero or one may indicate that one or more of the following situations exist:

- a. Extraneous noise is present in the measurements.
- b. The system relating $x(t)$ and $y(t)$ is not linear.
- c. The output $y(t)$ is due to other inputs besides $x(t)$.

3.6.2 Single-Input/Multiple-Output Models

Some of the basic principles obtained in the previous section will be used to formulate the FRF responses for single-input/multiple-output problems. It is assumed that the records used are from stationary random process with zero mean values and that the systems are constant-parameter linear systems. Figure 3.3 shows an example of a single-input/multiple-output system with extraneous output noise.

When the input signal $x(t)$ and the output signals $y_i(t)$ (where i is the number of output records in the system) are measured simultaneously, Bendat and Piersol defined the system response equation as:

$$G_{xy_i}(f) = H_i(f)G_{xx}(f) \quad (3.40)$$

where $G_{xy_i}(f)$ is the cross-spectral density of the input $x(t)$ and output $y_i(t)$, $G_{xx}(f)$ is the autospectral density of the input $x(t)$ and $H_i(f)$ is the frequency response function.

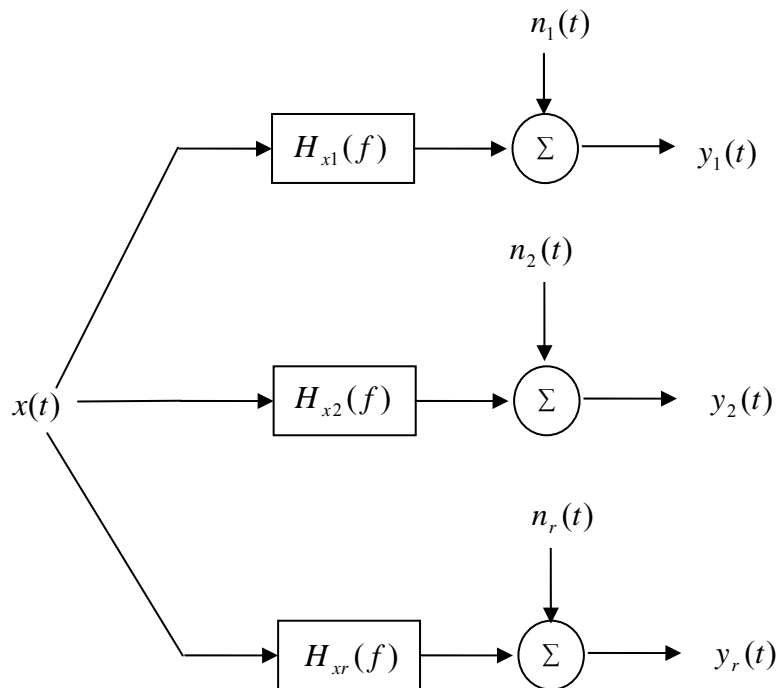


Figure 3.3 Single-Input/Multiple-Output System
(Adapted from Bendat/Piersol, 2000)

Thus, the FRFs for the system are obtained from:

$$H_i(f) = \frac{G_{xy_i}(f)}{G_{xx}(f)} \quad (3.41)$$

And the ordinary coherence function is defined as:

$$\gamma^2_{xy_i}(f) = \frac{|G_{xy_i}(f)|^2}{G_{xx}(f)G_{yiy_i}(f)} \quad (3.42)$$

3.7 Multiple-Input/Output Relationships

The previous system formulations and equations discussed will be extended to multiple-input/output problems in this section. It is assumed that all records are from stationary random process with zero mean values and that the systems are constant-parameter linear systems.

3.7.1 Multiple-Input/Single-Output Models

A set of q constant-parameter linear systems $H_i(f)$, $i = 1, 2, \dots, q$ with q clearly defined and measurable inputs $x_i(t)$, where $i = 1, 2, \dots, q$, and one measured output $y(t)$ is considered. Inputs may be mutually correlated. The output noise term $n(t)$ accounts for all deviations from the ideal model. These deviations may be due to unmeasured inputs, nonlinear operations, and instrument noise. Multiple-input/multiple-output models may be treated as a combination of separate and simpler multiple-input/single-output problems and can be solved using direct extensions of the techniques developed in this section. A multiple-input/single-input model is shown in Figure 3.4.

Four conditions must be satisfied in order to claim that the model is well-defined. These are stated by Bendat and Piersol as:

1. None of the ordinary coherence functions between any pair of input records should equal unity. If this occurs, the two input records contain redundant information and one of the input records should be eliminated from the model.
2. None of the ordinary coherence functions between any input and the total output should equal unity. If this occurs, then the other inputs are not contributing to this output and the model should be considered as a single-input/single-output model.

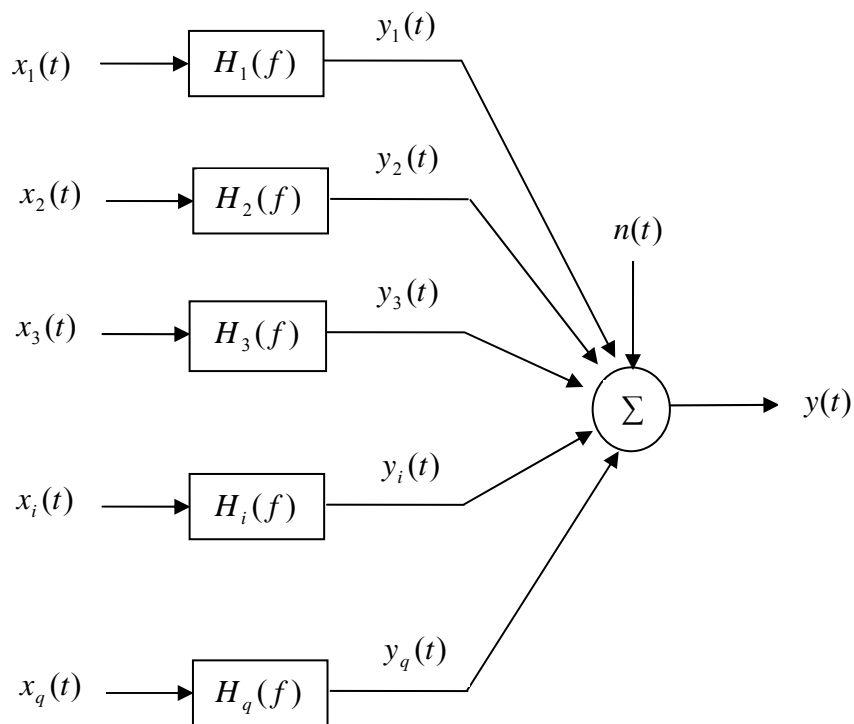


Figure 3.4 Multiple-Input/Single-Output System
(Adapted from Bendat/Piersol, 2000)

3. The multiple coherence function between any input and other inputs, excluding the given input, should not equal unity. If this occurs, then this input can be obtained by linear operations from the other inputs. Thus, this input is not providing any new information to the output and should be eliminated from the model.
4. The multiple coherence function between the output and the given inputs, in a practical situation, should be significantly high, which means above 0.50.

The output $y(t)$ may be considered to be the sum of the unmeasured q outputs $y_i(t)$, $i = 1, 2, \dots, q$ plus a noise term $n(t)$, as shown in the following equation

$$y(t) = \sum_{i=1}^q y_i(t) + n(t) \quad (3.43)$$

The corresponding finite Fourier transforms are:

$$Y(f) = \sum_{i=1}^q Y_i(f) + N(f) \quad (3.44)$$

Each output term $Y_i(f)$ for $i = 1, 2, \dots, q$ in Equation 3.44 satisfies the relationship shown:

$$Y_i(f) = H_i(f)X_i(f) \quad (3.45)$$

Therefore, the following equation can be defined

$$Y(f) = \sum_{i=1}^q H_i(f)X_i(f) + N(f) \quad (3.46)$$

where each $X_i(f)$ and $Y_i(f)$ is computed from the measured input signal $x_i(t)$ and the output signals $y(t)$.

The finite Fourier transforms for single records $x_i(t)$ and $y(t)$ of length T are

$$X_i(f) = \int_0^T x_i(t) e^{-j2\pi ft} dt \quad (3.47)$$

$$Y(f) = \int_0^T y(t) e^{-j2\pi ft} dt \quad (3.48)$$

The one-sided autospectral and cross-spectral density functions may be obtained using Finite Fourier Transforms instead of correlation functions.

$$G_{ii}(f) = G_{x_i x_i}(f) = \lim_{T \rightarrow \infty} \frac{2}{T} E[|X_i(f)|^2] \quad (3.49)$$

$$G_{ij}(f) = G_{x_i x_j}(f) = \lim_{T \rightarrow \infty} \frac{2}{T} E[X_i^*(f) X_j(f)] \quad (3.50)$$

$$G_{yy}(f) = \lim_{T \rightarrow \infty} \frac{2}{T} E[|Y(f)|^2] \quad (3.51)$$

$$G_{iy}(f) = G_{x_i y}(f) = \lim_{T \rightarrow \infty} \frac{2}{T} E[X_i^*(f) Y(f)] \quad (3.52)$$

In practice, only estimates of Equations (3.49) to (3.52) can be obtained, since T will be finite and the expected value operation $E[]$ can be taken only over a finite number of sample records.

When the records are digitized, the results will be obtained only at selected discrete frequencies. If the estimate of $G_{xy}(f)$ is denoted as $\hat{G}_{xy}(f)$, then at any frequency, f , the following relationship can be used (Bendat and Piersol):

$$\hat{G}_{xy}(f) = \frac{2}{n_d T} \sum_{k=1}^{n_d} X_k^*(f) Y_k(f) \quad (3.53)$$

where n_d is the number of different sample records $x(t)$ and $y(t)$, each of length T , so that the total record length $T_t = n_d T$. To reduce any bias errors, T should be made as large as possible. In addition, n_d should be as large as possible to reduce random errors.

Time-domain equations can be written involving the convolution integrals of the respective weighting functions $h_i(\tau)$, $i = 1, 2, \dots, q$, that are associated with the $H_i(f)$. Since using Fourier transforms in spectral relations is much simpler than using convolution integrals, Fourier transforms will now be used in order to obtain the desired quantities from this point.

For the general case of arbitrary inputs, if a different index of summation j is used instead of i in equation (3.46), then the following expression can be obtained.

$$Y(f) = \sum_{j=1}^q H_j(f) X_j(f) + N(f) \quad (3.54)$$

Multiplication of both sides by $X_i^*(f)$ for any fixed $i = 1, 2, \dots, q$ yields

$$X_i^* Y(f) = \sum_{j=1}^q H_j(f) X_i^* X_j(f) + X_i^* N(f) \quad (3.55)$$

where q is the number of inputs. If the expected values of both sides are taken then:

$$E[X^*_i(f)Y(f)] = \sum_{j=1}^q H_j(f)E[X^*_i(f)X_j(f)] + E[X^*_i(f)N(f)] \quad (3.56)$$

Multiplying the expression with a scale factor of $(2/T)$ yields the following expression:

$$G_{iy}(f) = \sum_{j=1}^q H_j(f)G_{ij}(f) + G_{in}(f) \quad (3.57)$$

If the model is well-defined, one can solve this system for $H_i(f)$ using matrix techniques.

The total autospectral density function $G_{yy}(f)$ can be written as:

$$\begin{aligned} G_{yy}(f) &= \sum_{i=1}^q \sum_{j=1}^q H^*_i(f)H_j(f)G_{ij}(f) + G_{nn}(f) \\ &+ \sum_{i=1}^q H^*_i(f)G_{in}(f) + \sum_{j=1}^q H_j(f)G_{nj}(f) \end{aligned} \quad (3.58)$$

assuming that the noise term $n(t)$ may be correlated with each input $x_i(t)$.

3.7.1.1 Two-Input/One-Output Models

The simplest case of multiple-input/single-output problems is two-input/one-output case. This case will be illustrated in this section in order to provide a better understanding of the theoretical approach presented above. A simple two-input/one-output system is

shown in Figure 3.5. The two-input/one-output system is defined by the basic transform relation

$$Y(f) = H_1(f)X_1(f) + H_2(f)X_2(f) + N(f) \quad (3.59)$$

Using the above equations, the following cross-spectral density functions between $x_1(t)$ and $y(t)$, and between $x_2(t)$ and $y(t)$, can be written as the following (dependency on frequency is omitted for simplicity).

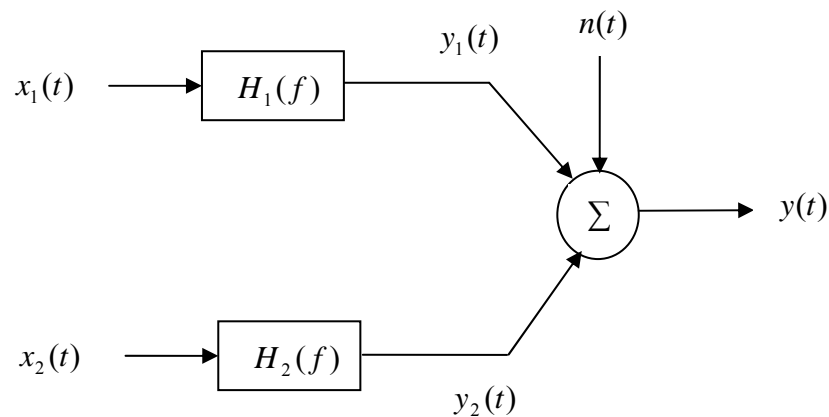


Figure 3.5 Two-Input/One-Output System with Output Noise
(Adapted from Bendat/Piersol, 2000)

$G_{11} = G_{11}(f)$ = autospectrum of $x_1(t)$

$G_{22} = G_{22}(f)$ = autospectrum of $x_2(t)$

$G_{yy} = G_{yy}(f)$ = autospectrum of $y(t)$

$G_{12} = G_{12}(f)$ = cross-spectrum between $x_1(t)$ and $x_2(t)$

$G_{1y} = G_{1y}(f)$ = cross-spectrum between $x_1(t)$ and $y(t)$

$G_{2y} = G_{2y}(f)$ = cross-spectrum between $x_2(t)$ and $y(t)$

$$G_{1y} = H_1 G_{11} + H_2 G_{12} + G_{1n} \quad (3.60)$$

$$G_{2y} = H_1 G_{21} + H_2 G_{22} + G_{2n} \quad (3.61)$$

If the noise term $n(t)$ is uncorrelated with each input $x_i(t)$, then G_{1n} and G_{2n} in Equation (3.60) and (3.61) will be zero.

The solution for $H_1(f)$ and $H_2(f)$, which assumes $\gamma^2_{12}(f) \neq 1$ and $G_{1n} = G_{2n} = 0$, is defined by Bendat and Piersol as:

$$H_1(f) = \frac{G_{1y}(f) \left[1 - \frac{G_{12}(f)G_{2y}(f)}{G_{22}(f)G_{1y}(f)} \right]}{G_{11}(f) [1 - \gamma^2_{12}(f)]} \quad (3.62)$$

$$H_2(f) = \frac{G_{2y}(f) \left[1 - \frac{G_{21}(f)G_{1y}(f)}{G_{11}(f)G_{2y}(f)} \right]}{G_{22}(f) [1 - \gamma^2_{12}(f)]} \quad (3.63)$$

with the ordinary coherence function

$$\gamma^2_{12}(f) = \frac{|G_{12}(f)|^2}{G_{11}(f)G_{22}(f)} \quad (3.64)$$

For the special case of uncorrelated inputs when $\gamma^2_{12}(f) = 0$, the terms $G_{12}(f)$ and $G_{21}(f)$ are zero also. The system can be reduced to a single-input/single-output model. For this special case, the following equations can be obtained:

$$H_1(f) = \frac{G_{1y}(f)}{G_{11}(f)} \quad (3.65)$$

$$H_2(f) = \frac{G_{2y}(f)}{G_{22}(f)} \quad (3.66)$$

3.7.1.2 Multiple Coherence Functions

A multiple coherence function is a direct extension of the ordinary coherence function. By definition, it is the ratio of the ideal output spectrum due to the measured inputs in the absence of noise to the total output spectrum, which includes the noise. In equation form, the multiple coherence function can be expressed by the following equation:

$$\gamma^2_{y:x}(f) = \frac{G_{vv}(f)}{G_{yy}(f)} = 1 - \left[\frac{G_{mm}(f)}{G_{yy}(f)} \right] \quad (3.67)$$

The ideal output spectrum may be written as $G_{vv}(f) = G_{yy}(f) - G_{mm}(f)$, where $G_{yy}(f)$ is provided in Equation (3.58).

Using Equation (3.67), the following relationship can be obtained.

$$G_{vv}(f) = \gamma^2_{y:x}(f)G_{yy}(f) \quad (3.68)$$

For all values of f , the multiple coherence function satisfies the following:

$$0 \leq \gamma^2_{y;x}(f) \leq 1 \quad (3.69)$$

If the multiple coherence function is zero, then $G_{vv}(f) = G_{yy}(f)$. This situation means that none of the output record comes from linear operations on the measured input records. The value unity indicates a perfectly linear model.

For a two-input/one-output model with uncorrelated inputs, the multiple coherence function is the sum of the ordinary coherence functions between each input and the output. This simple relation doesn't exist for correlated inputs. Thus, for uncorrelated inputs

$$\gamma^2_{y;x}(f) = \gamma^2_{1y}(f) + \gamma^2_{2y}(f) \quad (3.70)$$

3.7.1.3 Conditioned Spectral Density Functions

If correlation exists between any pair of input records, then it needs to be determined if one record causes part or all of the second record. Consider a two-input model where $x_1(t)$ and $x_2(t)$ are correlated, but not perfectly correlated, such that the coherence between them at all frequencies is $0 < \gamma^2_{12} < 1$. Turning off the first record will remove the correlated parts from the second record and leave only the part of the second record that is not due to the first record. Bendat and Piersol decomposed $x_2(t)$ into sum of two uncorrelated terms when any correlation between $x_1(t)$ and $x_2(t)$ comes from $x_1(t)$. This system can be seen in Figure 3.6.

$$x_2(t) = x_{2,1}(t) + x_{2,1}(t) \quad (3.71)$$

where $x_{2,1}(t)$ (called the residual or conditioned record) represents the part of $x_2(t)$ not due to $x_1(t)$. The optimum linear effect of $x_1(t)$ to $x_2(t)$ is denoted as $x_{2,1}(t)$.

The Fourier transform of Equation (3.71) yields

$$X_2(f) = X_{2,1}(f) + X_{2,1}(f) \quad (3.72)$$

where

$$X_{2,1}(f) = L_{12}(f)X_1(f) \quad (3.73)$$

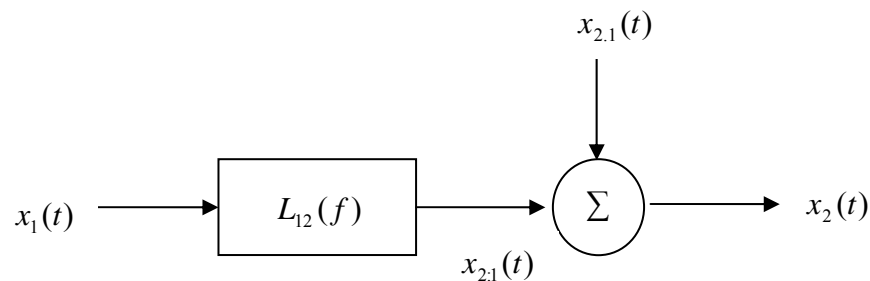


Figure 3.6 Decomposition of $x_2(t)$ from $x_1(t)$
(Adapted from Bendat/Piersol, 2000)

Equation (3.72) may then be written as

$$X_{2,1}(f) = X_2(f) - L_{12}(f)X_1(f) \quad (3.74)$$

The constant-parameter linear system $L_{12}(f)$ represents the optimum linear system used to predict $x_2(t)$ from $x_1(t)$ taken in that order. $L_{12}(f)$ is given by the ratio of the cross-spectrum from input to output divided by the autospectrum of the input, which can be defined as:

$$L_{12}(f) = \frac{G_{12}(f)}{G_{11}(f)} \quad (3.75)$$

The spectrum of $x_2(t)$ may also be decomposed into two parts as shown

$$G_{22}(f) = G_{22,1}(f) + G_{22,2}(f) \quad (3.76)$$

where $G_{22,1}(f)$ is the coherent output spectrum

$$G_{22,1}(f) = |L_{12}(f)|^2 G_{11}(f) = \gamma^2_{12}(f) G_{22}(f) \quad (3.77)$$

and $G_{22,2}(f)$ is the noise output spectrum

$$G_{22,2}(f) = [1 - \gamma^2_{12}(f)] G_{22}(f) \quad (3.78)$$

There are two approaches that are suggested for ordering the records. When no physical basis exists, a recommended approach is to compute the ordinary coherence function between each input record and the output record. The input signal giving the highest coherence is then selected as the first one. Another approach is to compute the cross-correlation function between the records to search for relative time delay.

In order to illustrate the procedures explained until this point, a simple two-input/one-output model will be analyzed. It is assumed that the input signals are correlated and $x_2(t)$ follows $x_1(t)$. The output of the system is denoted as $y(t)$. The inputs $x_1(t)$ and $x_{2,1}(t)$ are uncorrelated in the Figure 3.7. The constant-parameter linear system $L_{1,y}(f)$ is the optimum linear system to predict $y(t)$ from $x_1(t)$, whereas the constant-parameter linear system $L_{2,y}(f)$ is the optimum linear system to predict $y(t)$ from $x_{2,1}(t)$. In equation form, Figure 3.7 can be expressed as

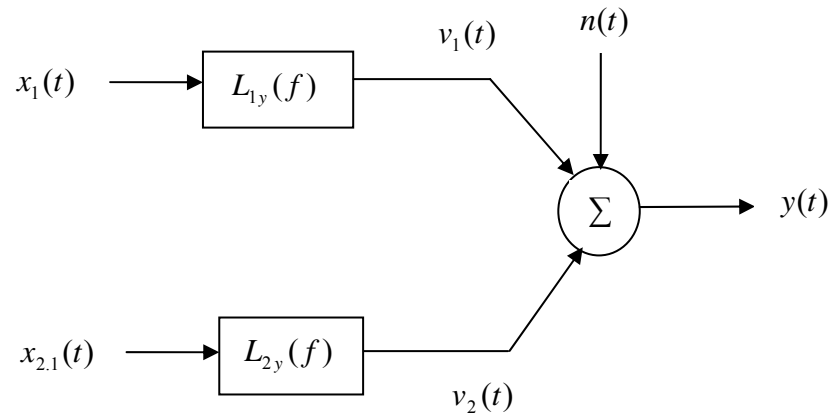


Figure 3.7 Two-Input/One-Output Model with Mutually Uncorrelated Inputs
 (Adapted from Bendat/Piersol, 2000)

$$Y(f) = L_{1y}(f)X_1(f) + L_{2y}(f)X_{2,1}(f) + N(f) \quad (3.79)$$

$$L_{1y}(f) = \frac{G_{1y}(f)}{G_{11}(f)} \quad (3.80)$$

$$L_{2y}(f) = \frac{G_{2y,1}(f)}{G_{22,1}(f)} \quad (3.81)$$

where the quantities

$G_{1y}(f)$ = cross-spectrum between $x_1(t)$ and $y(t)$

$G_{11}(f)$ = autospectrum of $x_1(t)$

$G_{2y,1}(f)$ = cross-spectrum between $x_{2,1}(t)$ and $y(t)$

$G_{22,1}(f)$ = autospectrum of $x_{2,1}(t)$

The quantity $G_{2y.1}(f)$ is called a conditioned (residual) cross-spectral density function, and $G_{22.1}(f)$ is called a conditioned (residual) autospectral density function. These functions are defined by Bendat and Piersol as

$$G_{2y.1}(f) = \frac{2}{T} E[X_{2.1}^*(f)Y(f)] \quad (3.82)$$

$$G_{22.1}(f) = \frac{2}{T} E[X_{2.1}^*(f)X_{2.1}(f)] \quad (3.83)$$

The frequency response functions for the system can then be obtained using the following relationship

$$L_{1y}(f) = H_{1y}(f) + L_{12}(f)H_{2y}(f) \quad (3.84)$$

$$L_{2y}(f) = H_{2y}(f) \quad (3.85)$$

There are only two unknowns in the above expressions ($H_{1y} = H_1$ and $H_{2y} = H_2$) and Equations (3.84) and (3.85) may be used to obtain these values. This process identified may be extended to solve multiple-input/output problems.

3.7.1.4 Partial Coherence Functions

In simplest terms, partial coherence functions play the same role as ordinary coherence functions, except that they apply to conditioned records instead of to the original records.

In partial coherence functions (the following assumes a two-input/one-output model):

1. Original records $x_1(t)$ and $y(t)$ are replaced by conditioned records $x_{2,1}(t)$ and $y_{y,1}(t)$.
2. Original spectral quantities $G_{11}(f)$, $G_{yy}(f)$ and $G_{1y}(f)$ are replaced by conditioned spectral quantities $G_{22,1}(f)$, $G_{yy,1}(f)$ and $G_{2y,1}(f)$.
3. The ordinary coherence function $\gamma^2_{1y}(f)$ is replaced by the partial coherence function $\gamma^2_{2y,1}(f)$.

Therefore, the ordinary function formula for input $x_1(t)$ and output $y(t)$ can be obtained as

$$\gamma^2_{1y}(f) = \frac{|G_{1y}(f)|^2}{G_{11}(f)G_{yy}(f)} \quad (3.86)$$

while the partial coherence function can be stated as

$$\gamma^2_{2y,1}(f) = \frac{|G_{2y,1}(f)|^2}{G_{22,1}(f)G_{yy,1}(f)} \quad (3.87)$$

For all values of f , the partial coherence function satisfies the following:

$$0 \leq \gamma^2_{2y,1}(f) \leq 1 \quad (3.88)$$

3.7.2 General and Conditioned Multiple-Input Models

The general multiple-input/output model for an arbitrary number of inputs is illustrated in Figure 3.8 and is adapted from “Random Data Analysis and Measurement Procedures (2000)” by Bendat and Piersol. The terms $X_i(f)$, $i = 1, 2, \dots, q$, where q is the number of

inputs records, represents the finite Fourier transforms of input signals $x_i(t)$. The finite Fourier transform of output record $y(t)$ is represented by $Y(f)$. The constant-parameter linear frequency response functions to be determined are represented by $H_{iy}(f), i=1,2,\dots,q$, while $N(f)$ represents the finite Fourier transform of the unknown extraneous output noise. It is assumed that the input and output records are measured simultaneously using a common time base.

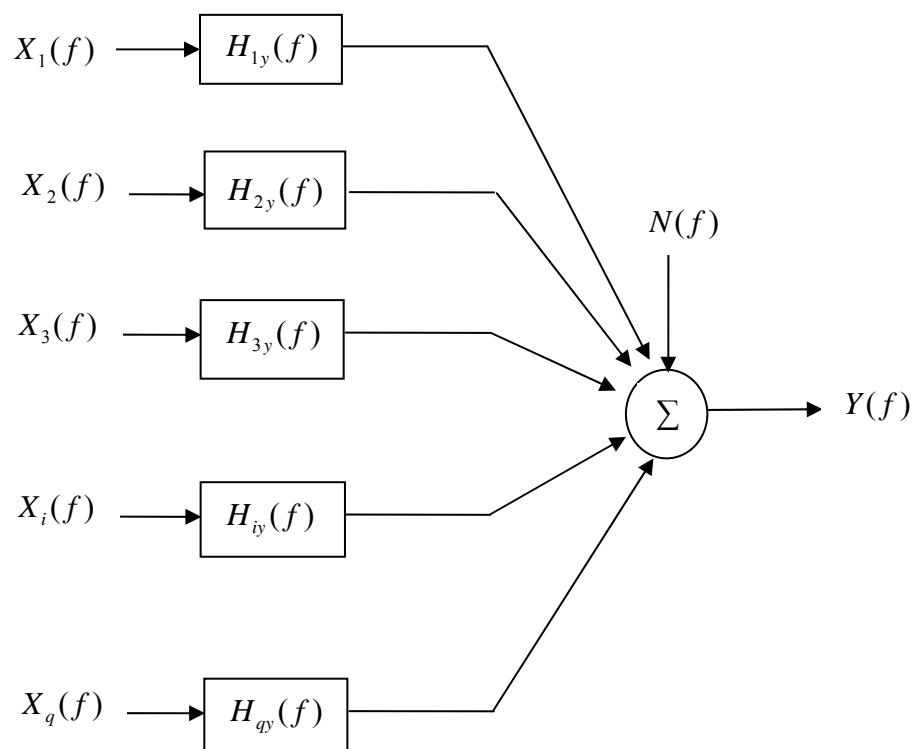


Figure 3.8 Multiple-Input Model for Arbitrary Inputs
(Adapted from Bendat/Piersol, 2000)

An alternate conditioned multiple-input/output model is shown in Figure 3.9. The original given inputs in previous figure are replaced by an ordered set of conditioned input records. For any i , the subscript notation $i.(i-1)!$ represents the i^{th} record conditioned on the previous $(i-1)$ records, which means that the linear effects of $x_1(t)$, $x_2(t)$, up to $x_{i-1}(t)$ have been removed from $x_i(t)$. These ordered conditioned input records will be mutually uncorrelated. Constant-parameter linear frequency response functions to be determined are represented by $L_{iy}(f)$, $i = 1, 2, \dots, q$, where the input precedes the output index.

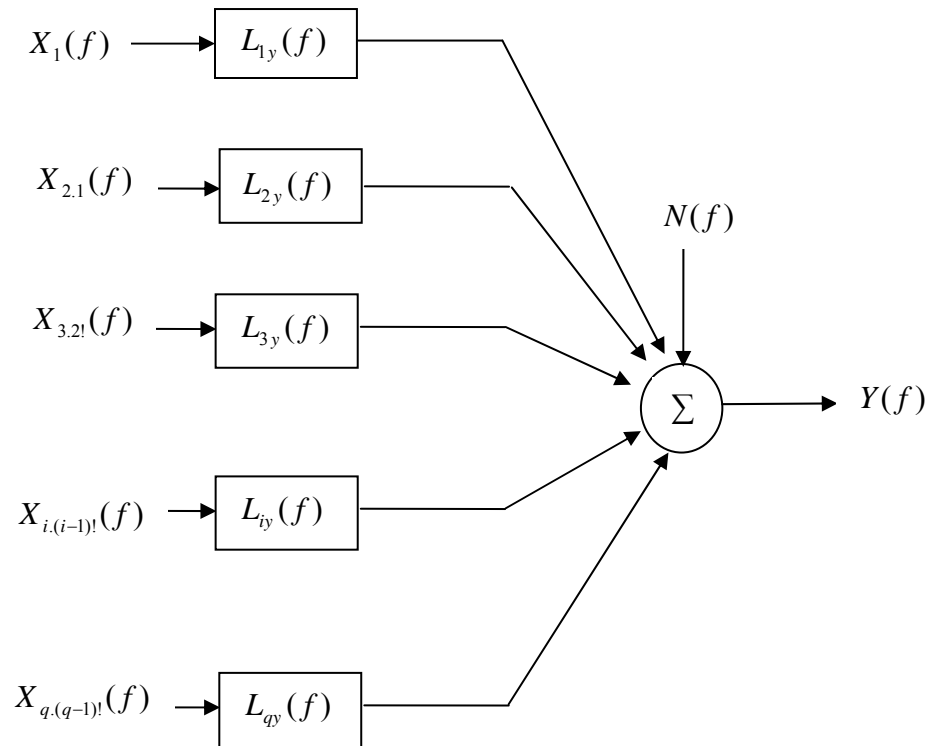


Figure 3.9 Multiple-Input Model for Ordered Conditioned Inputs
(Adapted from Bendat/Piersol, 2000)

3.7.2.1 Algorithm for Conditioned Spectra and Frequency Response Functions

A simple algorithm that computes frequency response functions from conditioned spectral densities was defined by Bendat and Piersol. A four-input/one-output problem which represents the multiple-input case of the benchmark problem is solved in order to illustrate this procedure in this section. Any multiple-input/multiple-output problem may be solved using the same algorithm by first breaking down the system into multiple-input/single-output problems and then ordering the signals using coherence functions.

The Fourier transforms of the conditioned inputs records are denoted by X_1 , $X_{2,1}$, $X_{3,2}$ up to $X_{q,(q-1)}$, where q is the number of input signals and may be calculated from the given input records by using the following formulation.

$$X_{j,r!} = X_{j,(r-1)!} - L_{rj} * X_{r,(r-1)!} \quad (3.89)$$

where j index must always be greater than r index, since only linear effects of a previous signal may be removed from a latter one. Equation (3.89) can be written for a four-input/one-output system as follows:

$$X_{2,1} = X_2 - L_{12} * X_1 \quad (3.90)$$

$$X_{3,2!} = X_{3,1} - L_{23} * X_{2,1} \quad (3.91)$$

$$X_{4,3!} = X_{4,2!} - L_{34} * X_{3,2!} \quad (3.92)$$

The constant-parameter linear system L_{qy} may be obtained as

$$L_{qy} = \frac{G_{qy,(q-1)!}}{G_{qq,(q-1)!}} \quad (3.93)$$

where the conditioned spectral density functions can be computed with the following expression

$$G_{ij,r!} = G_{ij,(r-1)!} - \left[\frac{G_{rj,(r-1)!}}{G_{rr,(r-1)!}} \right] G_{ir,(r-1)!} \quad (3.94)$$

If Equation (3.94) is examined carefully, it can be seen that the term $\frac{G_{rj,(r-1)!}}{G_{rr,(r-1)!}}$ is the same term in Equation (3.93) with different indices. Therefore, it may be calculated as

$$L_{rj} = \frac{G_{rj,(r-1)!}}{G_{rr,(r-1)!}} \quad (3.95)$$

$$\text{where} \quad r = 1, 2, \dots, (j-1) \quad (3.96)$$

$$j = 1, 2, \dots, (q+1) \quad (3.97)$$

General frequency response functions may then be found using

$$H_{iy} = L_{iy} - \sum_{j=i+1}^q L_{ij} H_{jy} \quad i = (q-1), (q-2), \dots, 1 \quad (3.98)$$

$$H_{qy} = L_{qy}$$

For a four-input/single-output model, (such as the benchmark problem analyzed in next section) frequency response functions may be obtained using the algorithm discussed above.

To Compute **L1y**:

$$L_{1y} = \frac{G_{1y}}{G_{11}} \quad (3.99)$$

To Compute **L2y**:

$$L_{2y} = \frac{G_{2y.1}}{G_{22.1}} \quad (3.100)$$

where

$$G_{2y.1} = G_{2y} - L_{1y} * G_{21} \quad (3.101)$$

$$G_{22.1} = G_{22} - L_{12} * G_{21} \quad (3.102)$$

$$L_{12} = \frac{G_{12}}{G_{11}} \quad (3.103)$$

and L_{1y} can be obtained from the previous system.

To Compute **L3y**:

$$L_{3y} = \frac{G_{3y.2!}}{G_{33.2!}} \quad (3.104)$$

where

$$G_{3y.2!} = G_{3y.1} - L_{2y} * G_{32.1} \quad (3.105)$$

$$G_{33.2!} = G_{33.1} - L_{23} * G_{32.1} \quad (3.106)$$

To Compute L_{4y} :

$$L_{4y} = \frac{G_{4y,3!}}{G_{44,3!}} \quad (3.107)$$

According to Equation (3.98), for a four-input / single-output model the relationship between constant-parameter linear systems H_{qy} and L_{qy} may be stated as:

$$H_{4y} = L_{4y} \quad (3.108)$$

$$H_{3y} = L_{3y} - L_{34}H_{4y} \quad (3.109)$$

$$H_{2y} = L_{2y} - L_{23}H_{3y} - L_{24}H_{4y} \quad (3.110)$$

$$H_{1y} = L_{1y} - L_{12}H_{2y} - L_{13}H_{3y} - L_{14}H_{4y} \quad (3.111)$$

3.7.2.2 Spectral Density and Frequency Response Functions Using Matrix Calculations

Let X be a column vector representing the Fourier transforms of the q input records $X_i = X_i(f)$, $i = 1, 2, \dots, q$ and Y be a column vector representing the Fourier transforms of the q output records $Y_k = Y_k(f)$, $k = 1, 2, \dots, q$

$$\begin{array}{r}
 X1 \\
 X2 \\
 \dots \\
 Xq
 \end{array}
 =
 \begin{array}{r}
 Y1 \\
 Y2 \\
 \dots \\
 Yq
 \end{array}
 \quad (3.112)$$

$$G_{xx} = \frac{2}{T} E\{X^* X'\} = \text{input spectral density matrix} \quad (3.113)$$

$$G_{yy} = \frac{2}{T} E\{Y^* Y'\} = \text{output spectral density matrix} \quad (3.114)$$

$$G_{xy} = \frac{2}{T} E\{X^* Y'\} = \text{input / output cross-spectral density matrix} \quad (3.115)$$

The basic matrix terms may be written using the definitions given above as follows

$$G_{xx} = \begin{matrix} G_{11} & G_{12} & \cdots & G_{1q} \\ G_{21} & G_{22} & \cdots & G_{2q} \\ \cdots & \cdots & \cdots & \cdots \\ G_{q1} & G_{q2} & & G_{qq} \end{matrix} \quad \text{input spectral density matrix} \quad (3.116)$$

$$G_{yy} = \begin{matrix} G_{y1y1} & G_{y1y2} & \cdots & G_{y1yq} \\ G_{y2y1} & G_{y2y2} & \cdots & G_{y2yq} \\ \cdots & \cdots & \cdots & \cdots \\ G_{yqy1} & G_{yqy2} & & G_{yqyq} \end{matrix} \quad \text{output spectral density matrix} \quad (3.117)$$

$$G_{xy} = \begin{matrix} G_{1y1} & G_{1y2} & \cdots & G_{1yq} \\ G_{2y1} & G_{2y2} & \cdots & G_{2yq} \\ \cdots & \cdots & \cdots & \cdots \\ G_{qy1} & G_{qy2} & & G_{qyq} \end{matrix} \quad \text{cross-spectral density matrix} \quad (3.118)$$

Without any further proof, the frequency response function matrix may be defined as follows

$$H_{xy} = G_{xx}^{-1} G_{xy} \quad (3.119)$$

where G_{xx}^{-1} is the inverse matrix of G_{xx} .

It is assumed that the number of inputs is the same as number of outputs and the inverse matrix operations can be performed.

Thus, the frequency response matrix obtained using Equation (3.119) can be shown as

$$H_{xy} = \begin{matrix} H_{1y1} & H_{1y2} & \dots & H_{1yq} \\ H_{2y1} & H_{2y2} & \dots & H_{2yq} \\ \dots & \dots & \dots & \dots \\ H_{qy1} & H_{qy2} & & H_{qyq} \end{matrix} \quad \text{frequency response matrix} \quad (3.120)$$

Multiple-input/multiple-output problems can be solved easily using the matrix techniques described above. However, for the greatest physical insight into the problem, it is recommended by Bendat and Piersol that these problems be broken down into multiple-input/single-output models, and solved by the algebraic procedures outlined in section 3.7.2.1.

Matrix calculations may also be used for multiple-input/single-output and single-input/single-output problems.

3.7.2.3 Partial and Multiple Coherence Functions

Ordinary coherence functions between any input $x_i(t)$ for $i = 1, 2, \dots, q$ and the total output y are defined by

$$\gamma^2_{iy}(f) = \frac{|G_{iy}(f)|^2}{G_{ii}(f)G_{yy}(f)} \quad (3.121)$$

Partial coherence functions between any conditioned input $x_{i,2!}$ for $i = 3, 4, \dots, q$ and the output $y,2!$ may be defined by the following expression

$$\gamma^2_{iy,2!} = \frac{|G_{iy,2!}|^2}{G_{ii,2!}G_{yy,2!}} \quad (3.122)$$

up to

$$\gamma^2_{qy,(q-1)!} = \frac{|G_{qy,(q-1)!}|^2}{G_{qq,(q-1)!}G_{yy,(q-1)!}} \quad (3.123)$$

where, for a q -input/one-output model, $G_{yy,q!}$ is called the noise output spectrum, and can be defined as

$$G_{yy,q!} = G_{yy} \prod_{i=1}^q (1 - \gamma^2_{iy,(i-1)!}) \quad (3.124)$$

Thus, for a two-input/one-output model, the noise output spectrum is

$$G_{yy,2!} = G_{yy,1}(1 - \gamma^2_{2y,1}) = G_{yy}(1 - \gamma^2_{1y})(1 - \gamma^2_{2y,1}) \quad (3.125)$$

For a q -input/one-output model, the multiple coherence function is given by

$$\gamma^2_{y:q!} = 1 - \left(\frac{G_{yy,q!}}{G_{yy}} \right) = 1 - \prod_{i=1}^q (1 - \gamma^2_{iy,(i-1)!}) \quad (3.126)$$

For a two-input/one-output model, the multiple coherence function may be defined by

$$\gamma^2_{y:2!} = 1 - \left(\frac{G_{yy,2!}}{G_{yy}} \right) = 1 - (1 - \gamma^2_{1y})(1 - \gamma^2_{2y,1}) \quad (3.127)$$